VRIJE
UNIVERSITEIT
BRUSSEL

Graduation thesis submitted in partial fulfillment for the degree of Master of Sciences in Applied Sciences and Engineering: Applied Computer Science

VALIDATING THE USE OF THE NINTENDO WII BALANCE BOARD FOR POSTURAL STEADINESS MEASUREMENTS IN THE TIME AND FREQUENCY DOMAINS.

Antonin Jousson

June 10, 2019

Promoter: Prof. Bart Jansen

Faculty of Engineering Sciences

"All truly great thoughts are conceived by walking."

Friedrich Nietzsche

Abstract

The biomechanics of the standing body are complex and minor balance disorders can lead to considerable health issues related to increased falling risks. The purpose of this study was to validate the use of the commercial Nintendo Wii Balance Board for balance assessment in static double limb standing conditions. The studied population was composed of six healthy adults and a specific measurement set up was used where the Wii Balance Board was placed on top of a gold standard AMTI force plate to allow for simultaneous recordings of the center of pressure displacements. 21 time domain and 18 frequency domain balance indicators were derived from the center of pressure displacements on both devices. Linear regressions, Bland-Altman plots and intraclass correlation coefficients were computed to assess the correspondence, agreement and reliability of the measurements. Our results indicate good to excellent reliability for previously validated time domain features and moderate to excellent reliability for the remaining ones. In the frequency domain, excellent reliability was found for features derived from the total power contained within the power spectrum while the other ones showed more mitigated results with reliability scores ranging from poor to good. Our findings bring evidence that we can partially extend the validity of the Wii Balance Board for balance assessment to measurements derived from the spectral analysis of the center of pressure displacement.

Acknowledgements

I would like to thank my thesis promoter Prof. Dr. Bart Jansen as well as Bruno Bonnechère for their knowledge, help and guidance which helped me successfully complete this research work. I would also like to express my gratitude towards my family, my friends, my classmates and finally my flatmates for their continuous support throughout the previous year and my studies in general.

Contents

List of Figures

List of Tables

Abbreviations

AP	**A**nterior **P**osterior
BA	**B**land **A**ltman
CNS	**C**entral **N**ervous **S**ystem
COP	**C**enter **O**f **P**ressure
DFT	**D**iscrete **F**ourier **T**ransform
FFT	**F**ast **F**ourier **T**ransform
FP	**F**orce **P**late
GRF	**G**round **R**eaction **F**orce
HS	**H**ealthy **S**ubjects
ICC	**I**ntraclass **C**orrelation **C**oefficient
ML	**M**edial **L**ateral
MS	**M**ultiple **S**clerosis
ODR	**O**rthogonal **D**istance **R**egression
PCS	**P**ostural **C**ontrol **S**ystem
PSD	**P**ower **S**pectral **D**ensity
RD	**R**esultant **D**istance
SWARII	**S**liding **W**indow **A**verage with **R**elevance **I**nterval **I**nterpolation
RMS	**R**oot **M**ean **S**quare
TLS	**T**otal **L**east **S**quare
TOB	**T**est **O**f **B**alance
WBB	**W**ii **B**alance **B**oard

Chapter 1

Introduction

1.1 Background and problem statement

According to Darwin's theory of evolution, human beings are primates who progressively evolved into bipeds by successive anatomical adaptations in response to environmental constraints. This transformation resulted in a complex postural control system (PCS) that plays a fundamental role in maintaining balance during the various activities we undertake in our daily life. Being able to maintain a stable posture is paramount as impaired balance is often a synonym of reduced functional ability [2]. The PCS is capable of maintaining balance thanks to the central nervous system (CNS) which constantly processes information from our main three sensory systems, namely the visual, vestibular, and proprioceptive systems [3, 4]. However, the aging process as well as various pathologies can affect this continuous feedback loop resulting in a degenerated balance control system [5]. Clinicians and researchers are constantly trying to increase their understanding of the PCS and discovering new methods to evaluate its performance [6].

There exists two different experimental paradigms for posturography: static, which assesses postural steadiness, and dynamic, which assesses postural stability [7]. As their names suggest, the first refers to the measurement of spontaneous sway movements of subjects standing on a flat, horizontal and stable surface whereas the dynamic paradigm focuses on the response of the PCS to external, pertubative and unpredictable stimuli [7]. In the static scenario, balance can be tested either qualitatively or quantitatively [2, 8]. The former is routinely done using subjective assessment tools, also called tests of balance (TOB). Those include, but are not limited to, the Timed get Up and Go test [9], the Tinetti Performance Oriented Mobility Assessment [10] and the Berg Balance Scale [11]. Such TOBs are convenient and can be easily performed in clinical settings since they do not require specific equipment yet they provide valuable information and

reliable data relative to postural steadiness and stability [12]. On the other hand, such qualitative protocols have known limitations such as ceiling and/or flooring effects [12] and "are usually not responsive enough to measure small progress or deterioration in a subject's ability to balance" [2]. The later is generally laboratory based and requires specific hardware, mostly force distribution plates (FP). Those devices are capable of recording the dynamic variation in the ground reaction force (GRF) along the contact phase with great precision using strain gauges transducers, allowing for accurate estimation of the center of pressure (COP) [8]. As such, they are often referred to as the "gold standard" for posturography [13] and are remarkable tools to explain body sway through estimation of various COP-based variables.

Unfortunately, force platforms come with their own set of disadvantages. With reported prices ranging from 5000 to 20000 euros, they are very onerous and cumbersome devices [14] which often need to be mounted at ground level to minimize noise, meaning they need to be embedded in the laboratory floor during experiments [15]. This kind of set up is obviously a huge limitation to the device's portability; not to mention they often require specific software and trained personnel [16]. The consequence is that they are inherently ill-fitted devices for in-field assessment of balance ability levels even though they remain the best option for laboratory usage.

Today there is a real and urgent need for a low-cost, portable and user-friendly balance assessment tool to complement the usual qualitative tests used in clinical diagnostics [12, 17, 18]. In 2006, Nintendo released the Nintendo Wii, a home video game console which met a huge success with the public because of its innovative approach towards gaming rooted in the stimulation of the player's body. One year later, Nintendo published the Wii Fit game along with its peripheral platform, the Nintendo Wii Balance Board. Initially designed as a video-game controller device, the Wii Balance Board (WBB) presents similarities with laboratory-grade force plates as it possesses four load cells from which the user's COP trajectory can be extracted [18]. Being mass-marketed and therefore widely available, considerably cheaper than force plates (less than 100 euros), lightweight and portable, it has been deemed the best candidate for balance training and diagnostic purposes by the clinical community [16]. Today, it is already put to use for postural steadiness assessment and has been integrated into rehabilitation programs of neurological patients with balance defects [12].

1.2 Contributions

Assessing the potential of the Wii Balance Board for low-cost posturography is not a brand new research topic in itself and there is a plethora of work that has already

been done in order to investigate the device's validity and usability by comparing it to force platforms. The classic approach followed by such studies is to measure COP related features using both devices and perform a statistical analysis of the data collected. However, most of the existing work focuses on balance estimators derived from the time series of the COP displacement; i.e time domain features. Very little work has been done to investigate the validity of the WBB for features measured in the frequency domain by performing a spectral analysis of the signal. Moreover, a signal processing method, which was specifically designed for the WBB has been published recently [1], but hasn't been integrated into many studies yet. Finally, most custom software written in the context of those validation studies is currently not open sourced. Based on those observations, the objectives of this work are threefold:

- Build upon existing validations studies by incorporating an exhaustive set of COP related features defined in the time and frequency domains.
- Integrate the open source implementation of the SWARII algorithm to the validation study.
- Facilitate further research by developing the building blocks of an open source python toolbox for low-cost posturography and, as a result, drive and ease adoption of such devices in clinical settings.

1.3 Thesis outline

This thesis is composed of five chapters. The opening chapter presents the context and purpose of our work as well as the targets in terms of contributions made to the field. The second chapter consists of a literature review which aims at exploring the currently existing approaches for low-cost posturography, focusing on studies using the Wii Balance Board and the associated state of the art methods. The third chapter is centered around the technicalities of the validation study we conducted. In a first part, we detail the material and methods used in our experiments. The statistical analysis performed is described in the second part. The results of our study are presented and extensively discussed in the fourth chapter. We conclude our work by summarizing the main outcomes of the study and by suggesting further investigations to be made in this research area.

Chapter 2

Related work

This chapter is dedicated to a review of the existing literature related to low-cost balance assessment. The emphasis is put on studies validating the Wii Balance Board as a potential proxy for force platforms in COP based balance assessment. By following a chronological approach, we try to draw an accurate and thorough picture of the experimental results landscape available today, from work conducted in the early days of the device up to the most recent advancements in the field.

Two years after the release of the Wii Balance Board to the public, Clark et al.[12] paved the way and published a paper that discusses the device's validity and reliability for assessment of standing balance. Moving away from research focusing on using the device for neurorehabilitation-based balance interventions, they pursued the objective of comparing the WBB COP quantification capabilities with a laboratory-grade force platform. Their validation study was based on 30 healthy subjects performing a "combination of single and double leg standing balance tests with eyes open or closed on two separate occasions" [12]. They used a single balance estimator for their comparison, the total COP path length. It is still unclear today what are the most relevant statistics to be computed in such studies to allow for meaningful comparison of the results. In their paper, Clark et al.[12] mention the use of intraclass correlation coefficients (ICC) and minimum detectable change (MDC) for between-device and within-device test-retest reliability as well as Bland-Altman plots (BAP) for inter-rater agreement. The results of their work "suggest that the WBB is a valid tool for assessing standing balance" [12]. It is important to notice that a calibration procedure was performed on the Wii Balance Board before the measurements.

Similar work was conducted by Hubbard et al.[19] with 18 healthy subjects. Here again, the COP path length was used as the primary balance estimator measure for between-device agreement validation using Bland Altman plots. Their results showed no major

trends or differences between the WBB and FP [19]. They also investigated the quality of the device's strain gauge transducers by performing calibration work similar to the one preconized by Clark et al.[12] and were able to demonstrate excellent linearity of the sensors [19].

Huurnink et al.[13] built upon Clark et al.[12] research with a comparison of WBB and FP COP data that was simultaneously collected during single leg standings by placing the WBB on top of a force platform [13]. The authors claim that such setup allows to retrieve simultaneous measurements and therefore eliminate within subject variability [13]. One important consequence is that a synchronization of the acquisition signals is needed afterwards to take into account the time lag induced by the setup. The authors used a method based on the time series covariance to remediate to this issue [13]. They included two COP based balance parameters in their analysis: the COP path velocity and the COP sway and used Pearson's correlation coefficient to quantify the correspondence of balance measurements between the WBB and the FP. Additionally, they computed the root mean square (RMS) error and Pearson's correlation coefficient for the COP trajectories in the x and y direction [13]. Their results showed high correlations and small differences in error between COP trajectories and high correlations for the two COP based aggregated balance measures [13]. Validating the linearity and consistency of measurements outcome on the COP trajectories was a big step forward as it "suggests that any balance measure based on a WBB COP trajectory can be considered sufficiently accurate" [13].

So far, the studies validated the WBB for balance assessment of healthy people. The work of Holmes et al.[20] targeted individuals suffering from Parkinson's disease. Their results, through excellent concurrent validity across balance tasks, brought the first evidence that the WBB could also be used on a population that present impaired balance due to a specific neurological condition [20].

Considering the initial purpose of the Wii Balance Board and its associated low-cost, one can legitimately ask themselves what is the quality of its sensors. Bartlett et al.[21] investigated the repeatability and accuracy of the WBB force and COP measurements under controlled static conditions in order to provide basic uncertainty metrics that are typically available for force plates [21]. They used 9 balance boards in total from which 3 were slightly used and 6 were heavily used. What came out of their study is that the total uncertainty of force measurements across boards is within ± 9.1 N and COP location within ± 4.1 mm [21]. Since "repeatability of a single measurement within a board was better (4.5 N, 1.5 mm)", it seems "that the WBB is best used for relative measures using the same device, rather than absolute measurement across devices" [21]. Nevertheless, those values are still way above the recommended uncertainty of 0.1 mm

for posturography applications [21]. On the other hand and perhaps more interestingly, the authors mention that those levels of uncertainty can be achieved using the internally stored factory calibration values of the WBB, allowing for off-the shelf usage [21]. Regarding the intensive use of the device, which is the case in clinical settings, it seems the WBB is rather well suited for high use situations since heavy wear did not significantly degrade performance [21].

Leach et al.[22] went one step further by undertaking a performance analysis under controlled dynamic conditions and assessed the impact of a custom linear calibration procedure on the WBB's COP signal accuracy [22]. Their results indicate that using a linear calibration procedure beforehand reduces COP measurement error and helps in the estimation of reliable time-domain COP measures [22]. The authors reported very low inter-device variability between the 12 different balance boards used in their study, corroborating the idea that the device should preferably be used for relative rather than absolute COP measurements.

Park et al.[18] added new evidence suggesting that the WBB is a suitable device for balance assessment in clinical settings. They performed a similar validation study to the ones from [12] and [13] on a set of 20 healthy adults. Not only did they obtain results that are in accordance with previous studies [18] as their findings show high inter-rater reliability, intra-rater reliability and concurrent validity of two COP based parameters, namely the COP path length and COP velocity; they also diminished the adoption barrier by developing a custom software that could facilitate the device's integration in clinical settings [18].

Shortly after, Sgrò et al.[23] performed a validation study where they "investigated the feasibility of the Wii Balance Board as an instrument for the assessment of balance and mobility proficiency in community-dwelling older people" [23]. Instead of comparing the WBB with a FP, they compared its discriminative power regarding ability levels of older people during balance and sit-to-stand tasks [23] with a widespread clinical test, the Short Physical Performance Battery (SPPB) test [24]. This is the first study that performed a comparison of quantitative and qualitative balance assessment approaches. The quantitative approach was based on the evaluation of an extended set of COP related posturography parameters compared to the previous studies. In total, they included eight parameters derived from the COP time series [23]. From a statistics point of view, they tested they hypothesis that the results of the SPPB test are in relation to the measures obtained from the WBB by means of a linear regression analysis [23]. A discriminant analysis was used for comparing the ability levels classification results of the clinical test and the low-cost gaming device [23]. In both cases, the levels of agreement were modest

but still promising as they outlined the potential of the WBB as a complementary tool to qualitative tests of balance in standing balance assessment [23].

We previously mentioned the work of Bartlett et al.[21] and, more specifically, their conclusions regarding the repeatability of measurements made with Wii Balance Boards. Bonnechère et al.[25] decided to go further in this direction by conducting an in-depth study of the interchangeability of the device in static postural assessment. While 12 WBBs were used by Bartlett et al.[21], the study was limited to a measurement uncertainty analysis using weights whereas Bonnechère et al.[25] compared simultaneous measurement of COP trajectories by a WBB and a FP (c.f [13] measurement protocol) using 4 different balance boards and this without applying any calibration procedure on the WBB. A total of nine parameters derived from the COP displacement were included in their statistical analysis in which they obtained good correlations between the balance boards as well as between the WBB and the FP [25]. Those findings are encouraging for multicenter studies and the creation of larger populations in clinical studies [25].

Aside from their study on the interchangeability of the WBB, Bonnechère et al.[25] conducted another validation study of the WBB, focusing this time on comparing the WBB with a FP for clinical evaluation of balance through different conditions [26]. Similarly to what was done in [25], simultaneous measurements by the WBB and a FP were collected using Huurnink et al.[13] protocol without any prior calibration of the WBB. They also used the same set of clinically relevant COP parameters in their analysis(nine in total). Their results suggest once more that the WBB and the FP have highly correlated measurements of COP based balance estimators [26]. Moreover, the authors claim that the correlations found between the two devices were better in the standing position (for both the single and double legs standing balance tests) than during the sitting balance tests [26].

Yoshikawa et al.[27] performed yet another study aiming at validating the usage of the WBB in stabilometry. Although the jargon used in this paper is slightly different from what we've been discussing so far, the work presented is still relevant in the context of this review. To clarify some terms, what they call "stabilometers" are equivalent to force platforms, "analysis indicators" or "analysis indices" refer to COP based balance estimators and "the total locus length" is a synonym of the total COP path length. The authors claim "previous comparisons of the Wii Balance Board and conventional stabilometers were performed using weight" and that "only the stabilograms were compared; there were no comparisons of practical analysis indices" [27]. Based on the preceding discussions from this chapter, this is not correct and suggests the authors did not carefully review the existing literature. Moreover, they mention calculations of balance estimators based on the center of gravity measurements, however, the WBB is only capable of measuring

the center of pressure. Those inaccuracies impel us to relate their conclusions with extra care. Nevertheless, their results tend to validate once again the good correlation of measurements between the WBB and force platforms, especially for the total locus length parameter [27]. Finally, the high number of subjects present in their study (102) adds statistical significance to their findings.

Monteiro-Junior et al.[17] made a contribution to the field by conducting a thorough evaluation of the WBB's reliability in static balance assessment of healthy elderly women. While they didn't adopt the comparative approach of previous studies, the added value of their work resides in the fact that they investigated both the within-day and between-day intra-rater reliability [17] on a specific population sample, namely elderly women. The outcomes of their statistical analysis revealed high ICCs in both scenarios. Considering that aging is the primary cause of falls and balance impairments, those findings reinforce the idea that the WBB could be used for periodic posture assessment in clinical settings on elderly people [17].

Castelli et al.[28] work was centered around a comparison of the WBB with traditional FP for balance assessment of patients suffering from multiple sclerosis (MS). Here again, the COP path length was the single COP related balance indicator extracted from the COP time domain series and on which the statistical analysis was based. Interpretation of the obtained ICC led the authors to conclude that between-device reliability of the WBB was just adequate while test-retest reliability was excellent [28]. However, they did not perform simultaneous measurements by superposition of the two devices which might have had an impact on the measurement variability [28]. On top of this, their results show that the WBB tends to overestimate postural sway when compared to force platforms [28] yet performs similarly to them when trying to discriminate fallers and non-fallers among patients with MS [28]. Those findings complement the ones from Bartlett et al.[21] and Bonnechère et al.[25] on the potential use of the device in multicenter studies. It is worth mentioning that the custom software used in this study, named "We-Measure"[1], was open sourced .

As stated before, multiple calibration techniques have been used to improve the quality of measurements obtained with a Wii Balance Board. Unfortunately this is not enough to solve one critical problem of the device: its inconsistent sampling rate. Audiffren and Contal.[1] tried to address this limitation by developing a new resampling method named SWARII that takes into account the non uniform acquisition rate of the WBB. The authors emphasize the importance of applying a correct resampling method that incorporates some kind of noise control mechanism as the WBB has a very high signal to noise ratio [1]. Considering the fact that the most important COP features for balance

[1] http://www.dia.uniroma3.it/~patrigna/portable_post/

assessment such as the COP velocity require to differentiate the COP time series [1], choosing an adequate resampling technique has a huge impact on the quality of the results. Their suggested approach to resampling is based on a sliding window average interpolation technique (SWAI) and complemented by the notion of relevance interval which acts as a regularization component and helps assigning correct weights to the data points based on the amount of noise present in the time window [1]. According to the authors, the SWARII generates results that are "significantly closer to the data obtained using [a] laboratory grade force platform AMTI" [1]. They provide an open source implementation[2] of the algorithm and recommend its usage in any work related to COP based balance assessment using Wii Balance Boards [1].

After having validated the interchangeability of the WBB [25] and its usage for balance assessment in different conditions [26], Bonnechère et al.[15] inspected the device performance regarding balance assessment during serious gaming rehabilitation exercises [15]. Similarly to the two previous studies, the WBB was superposed to a gold standard force platform and COP related balance estimators were measured without any prior calibration of the WBB [15]. The statistical analysis was based on nine parameters including displacement and velocities derived from the COP time domain series using ICC, Pearson correlation coefficients as well as Bland Altman plots. In line with what was found in the static scenario, overall good correlations were found between the WBB and the FP data [15].

The vast majority of the work discussed in the chapter make use of linear statistical tools on balance features derived from the COP displacements to assess the postural control system. Based on this observation Audiffren and Contal.[29] promoted the idea of building non linear models to classify fallers and non-fallers in elderly subjects [29]. For this reason, they used the highly non linear Ranking Forest algorithm to assign balance score, following a classical machine learning approach on a train-test split [29]. The Ranking Forest algorithm is a state of the art machine learning algorithm which relies internally on the aggregation of many weak decision trees classifiers, also known as the bagging technique, to obtain robust predictors. They trained the machine learning algorithm on a set of five descriptors that were derived from COP related features which have previously been studied and validated as potential predictors of future falls [29]. The data was collected on a WBB and, following their own recommendations [1], the authors resampled the signal using the SWARII resampling method [29]. The main takeaways from their Receiver Operating Characteristic (ROC) analysis is that, while each feature alone results in almost random performance in classifying fallers/non-fallers (with an Area Under Curve (AUC) ranging from 0.49 to 0.54), the multi dimensional approach resulted in much better classifying capabilities with an AUC of 0.75 [29] . Furthermore,

[2] https://reine.cmla.ens-cachan.fr/j.audiffren/SWARII

even if the authors did not open source their implementation at this time, an online version[3] of the algorithm has been made available.

Altough multiple previous studies already investigated the postural control assessment capabilities of the WBB on healthy subjects, Zakeri et al.[30] proceeded to a similar methodological validation study on twenty healthy people. Surprisingly enough, their analysis was limited to two COP based parameters only, namely the COP path length and the COP range in the AP direction. Overall, the authors estimated the levels of reliability found by means of ICC computations just "acceptable" while visual inspection of the Bland Altman reinforced the argument that the WBB measurements are comparable to FP ones even though the WBB has a tendency towards consistent overestimation of said parameters [30].

Severini et al.[16] work can be seen as an extension of Castelli et al.[28] considering they also investigated the usability of the WBB for balance assessment of Multiple Sclerosis(MS) patients. They assessed the validity and reliability of the device using 18 balance related features derived from the COP [16]. This is the first study to include so many features in a comparative study of the WBB and the FP. Having such a large amount of features at their disposal, they decided to use a machine learning approach using Support Vector Machine (SVM) based classifiers to assess the ability of both devices to discriminate between Healthy Subjects (HS) and MS [16]. Promising results were obtained since the classifiers trained on data extracted from the WBB showed similar performance (accuracy above 80%) to the ones trained on features extracted from the FP [16]. Overall, their findings were in line with what has been published before and corroborate the argument that "altough the WBB is not suitable for obtaining absolute measures, [it] could be successfully used in comparative analysis of different populations" [16].

At the end of 2017, Martinez et al.[14] took a look at the test-retest reliability of the WBB for postural steadiness measurements in young people with Intellectual Disability (ID). The test-retest reliability of the device had already been described as excellent in multiple previous studies [12, 21, 28] and this was also confirmed in this study for subjects presenting mild intellectual disability. On the other hand, some limitations were also brought out which suggest the "device might not be sensitive enough to properly identify static balance changes in [people with moderate/severe ID]".

Very recently, Van Hove et al.[31] reflected upon the possibility of assessing balance modifications induced by increased respiratory loads in healthy subjects [31]. The same set of time domain features related to COP displacement and speed as the ones previously validated in [15, 25, 26] were used. Even if the WBB was used in a standalone mode

[3] http://taureau.pppcmla.ens-cachan.fr/

(i.e no comparison with any FP was done), results were promising as they show "that substantial changes in balance control were captured by the WBB" [31]. More specifically, a linear relationship between the detected balance impairment and the amplitude of the inspiratory load was found [31].

Eight years after their previous work [12], Clark et al.[32] established a systematic review of 25 articles related to validation of the reliability and concurrent validity of the WBB for assessment of static standing balance. Their work highlights the fact that the WBB has proven itself as a reliable and valid tool for assessing standing balance [32]. Their conclusion is mostly the same as what the discussion from this chapter suggests. Nevertheless, it is obvious that there is a gap in evidence regarding the validity of the WBB for postural steadiness assessment using balance estimators computed in the frequency domain. Based on all the information gathered in this chapter, we fine tuned our own comparative study of the WBB with an AMTI FP to include an exhaustive set of features defined both in the time and frequency domains.

Chapter 3

Material and methods

In this chapter, we take a closer look at the material and methods used in our validation study. More particularly, we describe the study participants sample as well as the measurement protocol used to assess postural steadiness. We then outline the different stages of the data (pre)processing pipeline followed by the various methods used for the statistical analysis of the results.

3.1 Subjects and procedures

The data used in this study was already at our disposal and was generated in the context of previous research work on the interchangeability of the Wii Balance Board for balance assessment [25]. As such, the following description corresponds to the subjects and procedures mentioned in the preceding study.

3.1.1 Participants

Six healthy adults including four men and two women participated in the study. Table 3.1 indicates their mean age, height and weight.

Number of participants	Mean age	Mean height (cm)	Mean weight (kg)
6	36 (SD 13)	176 (SD 11)	81 (SD 22)

TABLE 3.1: Study participants sample summary.

3.1.2 Measurement setup

As in Huurnik et al.[13], the setup consisted of a Wii Balance Board put on top of a AMTI force plate (model OR6-6, Watertown, MA, USA, size 50 cm $\times$ 46 cm). The advantage of such setup is that it allows for simultaneous data retrieval and therefore eliminates within subject variability [13]. The force plate was embedded within the laboratory floor and had a sample rate of 1000 Hz. Four different Nintendo Wii Balance Boards (serial numbers BEH428405719, BEH428409281, BEH428408987, and BEH428409175) were used. The data acquisition was done using a Bluetooth connection between the balance boards and a laptop((Intel Core I5, Windows 7, 6 GB RAM) running a custom-written software based on the Wiimotelib software.

Even though there has been a few calibration methods proposed for the Wii Balance Board [12, 13, 22], none was used here since the purpose of the study was "to evaluate the repeatability of measurements ... without the practical constraint of such systematic calibration procedures" [25]. The force plate was calibrated beforehand following the manufacturer's recommendations [25].

3.1.3 Measurement protocol

A static posturography measurement protocol was used in the study where the participants were asked to perform three repetitions of double limb standing. More precisely, they had "to stand in the middle of the Wii Balance Board for 30 seconds, as motionless as possible, eyes open, arms aligned along the body, and eyes fixed on a target on the wall in front of them" [25]. All subjects went through three trials on each of the four Wii Balance Boards which resulted in a single session of twelve trials. A randomized process was used to come up with the order of the tested Wii Balance Board.

3.2 Data preprocessing

We applied the same preprocessing steps as in [25], namely computations of the displacements of the center of pressure along anterior-posterior (AP) and medial-lateral (ML) directions, resampling, filtering and detrending of the signal. However our approach to the Wii Balance Board data resampling step was significantly different since we decided to use the sliding window average with relevance interval interpolation (SWARII) algorithm as suggested by Audiffren and Contal [1] while linear interpolation was used by Bonnechère et al.[25]. We used the python bindings of the open source Biomechanical ToolKit [33] to extract data from the raw C3D acquisition files.

3.2.1 Center of pressure coordinates computations

The center of pressure (COP or CP) is the prevalent posturographic measure in the context of postural control assessment. It is defined as the "location of the vertical reaction vector on the surface of a force platform on which the subject stands" [34] and it "reflects the orientations of the body segments (joint angles), as well as the movements of the body (joint angular velocities and accelerations) to keep the center of gravity over the base of support" [34].

Both the Wii Balance Board and the AMTI force plate are able to measure the COP displacement. In our case, the WBB COP had already been computed by the custom software used during data acquisition but the exact methodology used wasn't reported. The force plate COP computations, however, were left for us to be done. The next paragraphs aim at describing those computations based on the most frequent methods found in the literature.

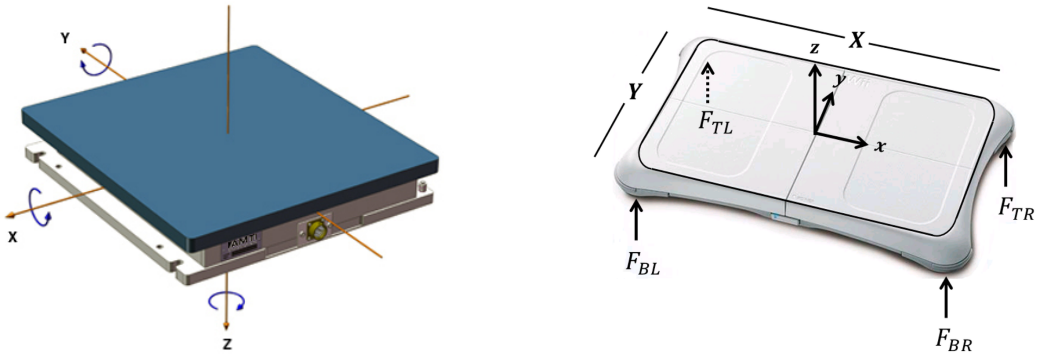

(A) Force plate (B) Wii Balance Board

FIGURE 3.1: Experimental apparatus.

- **Force plate**

  The force plate is able to measure the orthogonal force and torque components in the three spatial directions thanks to its four load cells force sensors. The x,y and z axis of the force plate are represented on Figure 3.1a and correspond to the anterior-posterior (AP), medial-lateral(ML), and vertical directions, respectively.

  Equation 3.1 gives the expression of the COP in both ML and AP directions based on the physical variables measured by the force plate:

$$COP_{ML}^{FP} = \frac{-M_x + d_z.F_y}{F_z}$$
$$COP_{AP}^{FP} = -\frac{M_y + d_z.F_x}{F_z} \tag{3.1}$$

where M_x and M_y represent the x and y axis torque components, F_x and F_y represent the x and y axis forces components and d_z is a constant corresponding to the thickness of the base of support above the FP surface.

- **Wii Balance Board**

  The Wii Balance Board is equipped with four gauge-strain sensors located beneath its surface. As we can see on Figure 3.1b, the sensors are placed in the corners of the device and are only capable of measuring the vertical component of the ground reaction force.

  Equation 3.2 gives the expression of the COP in both ML and AP directions based on the physical variables measured by the Wii Balance Board:

$$COP_{ML}^{WBB} = \frac{X}{2}.\frac{(F_{TR} + F_{BR}) - (F_{TL} + F_{BL})}{F_z}$$
$$COP_{AP}^{WBB} = \frac{Y}{2}.\frac{(F_{TR} + F_{TL}) - (F_{BR} + F_{BL})}{F_z} \tag{3.2}$$
$$F_z = F_{TR} + F_{TL} + F_{BR} + F_{BL}$$

  where F_{TL}, F_{TR}, F_{BL}, F_{BR} are the vertical component of the ground reaction force in the top left, top right, bottom left and bottom right corners of the WBB. X and Y represent the length and the width of the WBB as shown on Figure 3.1b.

3.2.2 Resampling

We previously mentioned in subsection 3.1.2 that the force plate frame rate acquisition was 1000 Hz. The Wii Balance Board, on the other hand, has an inconsistent sampling rate. This means the sampling frequency of the WBB is not constant and varies significantly throughout an acquisition. The different sampling regimes of the device are represented on Figure 3.2 which was taken from the work of Audifren and Contal [1]. We can see that "the WBB alternates between three different regimes: a fast paced regime ($<$ 100 Hz), a moderate regime ($\approx$ 54 Hz) and a slow regime ($\approx$ 35 Hz)" [1], with an average sampling frequency situated around 63 Hz.

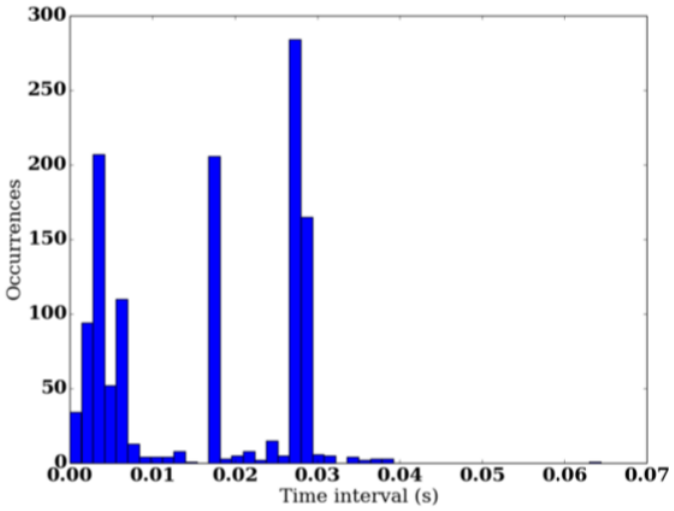

FIGURE 3.2: Repartition of time intervals between two consecutive data points recorded by the WBB during a 20 s record (taken from [1]).

Many resampling methods are available but a recent WBB specific solution proposed by Audifren and Contal [1] retained our attention. We used their open source implementation of the SWARII. We resampled both the FP and the WBB signals to a sample rate of 100 Hz. The SWARII was used on the WBB data using a time window length of 0.6 seconds (see Figure 4.3). The FP data was downsampled using a decimation method with a factor of 10 to match the WBB sampling frequency. The implementation used for the downsampling applies an anti-aliasing filter on the signal beforehand.

3.2.3 Additional preprocessing steps

The following additional preprocessing steps were performed on the force plate and the Wii Balance Board data:

- **Filtering and detrending**

  Our extensive review of the literature (see chapter 2) suggests that a low-pass Butterworth filter should be applied on the COP signal before further processing is done. An eight-order filter with a cut-off frequency of 12 Hz was used for the FP. The filtering step was omitted for the WBB "as doing averages over a window already denoises the signal" [1]. As suggested by [8], we also detrended the COP signal by removing the mean COP position in both AP and ML directions.

- **Time window selection and signal synchronization**

  The total acquisition time was around 30 seconds. We decided to take into account only the last 20 seconds of the signal since significant noise was present in the

beginning of the acquisition. This was attributed to participants standing on and off the set up. Because of the physical configuration of the experimental set up, a time lag was observed between the force plate and the Wii Balance Board signals. We adjusted the WBB and FP selected time windows to take this offset into account through visual inspection of the results. To the opposite of what Huurnink et al.[13] did, we unfortunately did not automate this synchronization step.

3.3 Data processing

Close inspection of the literature led us to extract a total of 39 COP-based features from which 21 were computed in the time domain and the remaining 18 were computed in the frequency domain. In the next paragraphs, we explicate the mathematical expressions used to derive the COP related parameters. As mentioned in the previous section, the time period selected for the analysis is $T = 20$ s. Considering the resampling frequency chosen of 100 Hz, this leads to a total of $N = 2000$ data points. The reader will find the source code of our python implementation in Appendix A.

3.3.1 Center of pressure time series

Let us consider the preprocessed COP coordinate time series in the ML and AP directions derived from subsection 3.2.1: $COP_{ML}[n]$ and $COP_{AP}[n]$ where $n = 1...N$. We can then define the resultant distance (RD) time series as:

$$COP_{RD}[n] = \sqrt{COP_{ML}[n]^2 + COP_{AP}[n]^2} \tag{3.3}$$

The RD time series corresponds to the vector distance from the mean COP to each pair of points in the AP and ML time series [34].

3.3.2 Time domain features

Posturographic measurements computed in the time domain are the prevalent type of measurements and are routinely used to measure the postural control system static performance. Time domain COP features can be classified in three measurement type categories: distance measures, area measures and hybrid measures. In the following paragraphs, equations are defined for the RD and ML time series but the ML time series

equations are also valid for AP time series and can be trivially derived by substituting the ML time series with the AP ones.

3.3.2.1 Distance measures

COP distance measures are the most common and basic ones. Parameters that are linked to the displacement of the COP from the central point of the stabilogram as well as COP velocity fall in this category.

- **Mean distance**

  Equation 3.4 defines the mean distance ($MDIST$) and mean distance-ML ($MDIST_{ML}$) parameters. The first one, which is defined as the mean of the RD time series, represents the average distance from the mean COP. The second one, which is defined as the mean absolute value of the ML time series, represents the average ML distance from the mean COP.

$$\begin{aligned} MDIST &= \frac{1}{N}\sum_{n=1}^{N} COP_{RD}[n] \\ MDIST_{ML} &= \frac{1}{N}\sum_{n=1}^{N} \mid COP_{ML}[n] \mid \end{aligned} \tag{3.4}$$

- **Root mean square distance**

  Equation 3.5 defines the $RDIST$ and $RDIST_{ML}$ parameters. They represent the root mean square distance from the mean COP.

$$\begin{aligned} RDIST &= \frac{1}{N}\sqrt{\sum_{n=1}^{N} COP_{RD}[n]^2} \\ RDIST_{ML} = SD_{ML} &= \frac{1}{N}\sqrt{\sum_{n=1}^{N} COP_{ML}[n]^2} \end{aligned} \tag{3.5}$$

- **Total excursions**

  Equation 3.6 defines the total excursions ($TOTEX$) and total excursions-ML ($TOTEX_{ML}$) parameters. They represent the total length of the COP path and the total length of the COP path in the ML direction respectively. Summing the distance between

consecutive points on the COP path and in the ML time series gives a good approximation of such parameters.

$$TOTEX = \sum_{n=1}^{N-1} \sqrt{(COP_{AP}[n+1] - COP_{AP}[n])^2 + (COP_{ML}[n+1] - COP_{ML}[n])^2}$$
$$TOTEX_{ML} = \sum_{n=1}^{N-1} \mid COP_{ML}[n+1] - COP_{ML}[n] \mid \tag{3.6}$$

- **Mean velocity** Equation 3.6 defines the mean velocity ($MVELO$) and mean velocity-ML ($MVELO_{ML}$) parameters. They represent the average velocity of the COP and the average velocity of the COP in the ML direction respectively.

$$MVELO = \frac{TOTEX}{T}$$
$$MVELO_{ML} = \frac{TOTEX_{ML}}{T} \tag{3.7}$$

- **Range**

  Equation 3.6 defines the range ($RANGE$) and range-ML ($RANGE_{ML}$) parameters. The range corresponds to the maximum distance between any two points on the COP path and the range-ML is the absolute value of the difference between the smallest and largest values in the ML time series [34].

$$RANGE = \max(COP_{RD}) - \min(COP_{RD})$$
$$RANGE_{ML} = \mid (\min(COP_{ML}) - \max(COP_{ML})) \mid \tag{3.8}$$

3.3.2.2 Area measures

COP area measures are also often found in the literature. Such parameters usually try to estimate the area enclosed by the stabilogram.

- **95 % confidence circle area**

  Equation 3.9 shows the expression of the 95 % confidence circle area. Starting from the assumption that the distances are normally distributed, we can model the area of the stabilogram with a circle that includes approximately 95 % of the distances

from the mean COP [34]. By construction, the radius of such circle is equal to the 95 % confidence limits of the RD time series.

$$AREA - CC = \pi(MDIST + Z_{0.5}SD_{RD})^2$$
$$SD_{RD} = \sqrt{\frac{1}{N}\sum_{n=1}^{N} COP_{RD}[n]^2 - MDIST^2} = \sqrt{RDIST^2 - MDIST^2} \tag{3.9}$$

where is the standard deviation of the RD time series and $Z_{0.5} = 1.645$ is the z statistic at the 95 % confidence level.

- **95 % confidence ellipse area**

  Another common area measure is the 95 % ellipse area. It is defined as the area of the 95 % bivariate confidence ellipse which encloses approximately 95 % of the points on the COP path [34]. Equation 3.10 defines the expression of the semi minor and semi major axes parameters for such an ellipse.

$$\begin{aligned} a &= \sqrt{F_{0.5[2,n-2]}(SD_{AP}^2 + SD_{ML}^2 + D)} \\ b &= \sqrt{F_{0.5[2,n-2]}(SD_{AP}^2 + SD_{ML}^2 - D)} \end{aligned} \tag{3.10}$$

  where $F_{0.5[2,n-2]} = 3.00$ is the F statistic at a 95 % confidence level for a bivariate distribution with n data points ($n > 120$). SD_{ML} and SD_{AP} are the ML and AP time series standard deviations.

$$\begin{aligned} D &= \sqrt{(SD_{AP}^2 + SD_{ML}^2) - 4(SD_{ML}^2 SD_{AP}^2 - SD_{APML}^2)} \\ SD_{APML} &= \frac{1}{N}\sum_{n=1}^{N} COP_{AP}[n]COP_{ML}[n] \end{aligned} \tag{3.11}$$

  where SD_{APML} is the covariance.

  The equation for the 95 % ellipse area is derived by combining Equation 3.10 and Equation 3.11:

$$AREA - CE = \pi ab = 2\pi F_{0.5[2,n-2]}\sqrt{SD_{AP}^2 SD_{ML}^2 - SD_{APML}^2} \tag{3.12}$$

3.3.2.3 Hybrid measures

The last and perhaps more exotic kind of COP parameters defined in the time domain are the hybrid measures. As the name suggests, hybrid measures are constructed by combining distance measures.

- **Sway Area**

  Equation 3.13 shows the expression of the Sway area ($AREA-SW$). It is an estimator of the area enclosed by the COP path per unit of time and is approximated by summing the area of the triangles formed by two consecutive points on the COP path and the mean COP [34].

$$AREA-SW = \frac{1}{2T}\sum_{n=1}^{N-1} \mid COP_{AP}[n+1]COP_{ML}[n] - COP_{AP}[n]COP_{ML}[n+1] \mid \tag{3.13}$$

- **Mean Frequency**

  Equation 3.14 shows the expression of the mean frequency ($MFREQ$) and the mean frequency-ML ($MFREQ_{ML}$). The mean frequency is the rotational frequency, in revolutions per second, of the COP if it had traveled the total excursions around a circle with a radius of the mean distance. The mean frequency-ML is the frequency, in Hz, of a sinusoidal oscillation with an average value of the mean distance-ML and a total path length of total excursions-ML [34].

$$\begin{aligned} MFREQ &= \frac{TOTEX}{2\pi TMDIST} = \frac{MVELO}{2\pi MDIST} \\ MFREQ_{ML} &= \frac{TOTEX_{ML}}{4\sqrt{2}MDIST_{ML}T} = \frac{MVELO_{ML}}{4\sqrt{2}MDIST_{ML}} \end{aligned} \tag{3.14}$$

- **Fractal Dimension**

  Equation 3.15 shows the expression of the fractal dimension, FD, which is a unitless measure of the capacity of a pattern to fill the metric space in which it is defined [34]. We computed two different fractal dimensions: the fractal dimension-CC and the fractal dimension-CE. The first one models the area of the stabilogram with the 95 % confidence circle described in Equation 3.9 and is computed by replacing d in Equation 3.15 with d_{FD-CC}. Similarly, fractal dimension-CE models the area of the stabilogram with the 95 % confidence ellipse described in Equation 3.12 and is computed by replacing d in Equation 3.15 with d_{FD-CE} [34].

$$FD = \frac{\log(N)}{\log(\frac{Nd}{TOTEX})} \tag{3.15}$$

$$d_{FD-CC} = 2(MDIST + Z_{0.5}SD_{RD}) \tag{3.16}$$

$$d_{FD-CE} = \sqrt{2a2b} = \sqrt{8F_{0.5[2,n-2]}\sqrt{SD_{AP}^2 SD_{ML}^2 - SD_{APML}^2}} \tag{3.17}$$

3.3.3 Frequency domain features

Even though time domain features have been extensively used and proven to be good balance estimators, frequency domain features based on the Fourier transform of the COP time series can also be found in the literature.

3.3.3.1 Power spectral density estimation

The first step in order to be able to compute features in the frequency domain is to do a Fourier analysis, also called spectral analysis, of the COP time series. The Fourier transform is formally defined as an integral transform. However, practically, the discrete Fourier transform (DFT) is commonly used to approximate the analytical solution on a finite sequence of equally-spaced samples. The most common implementation of the DFT, the fast Fourier transform algorithm (FFT), allows to quantify the signal power distribution over frequency, also known as the power spectral density (PSD) or power spectrum.

There are numerous ways to estimate the PSD that can be divided in two categories: parametric and non-parametric methods. We decided to apply the same non-parametric method as Prieto et al.[34], the sinusoidal multitaper method. Practically, we used python bindings [35] to the Fortran Multitaper Spectrum Estimation Library mwlib.a by Germán A. Prieto [36]. The units of the PSD, in the case of the COP displacement, are $\frac{mm^2}{Hz}$.

We stated in subsection 3.2.2 that the sampling frequency for this study was $f_{sampling} =$ 100 Hz. Based on the Nyquist-Shannon sampling theorem, the associated Nyquist frequency will be $f_{Nyquist} = f_{sampling}/2 = 50$ Hz, corresponding to the power spectrum bandwith B. However, we based our analysis on a reduced frequency range, going from 0.15 to 5.0 Hz. We removed the dc component and the next two frequency points after it since they were not deemed relevant for the study.

3.3.3.2 Frequency measures

The following measures are defined for each of the three COP times series (AP, ML and RD) and are obtained by substituting the corresponding discrete power spectral density estimates.

- **Spectral moments**

  Equation 3.18 defines the PSD spectral moments, μ_k, where $\Delta f = 0.05$ Hz is the frequency increment in the discrete power spectral density estimate $G[m]$.

$$\mu_k = \sum_{m=3}^{j=100} (m\Delta f)^k G[m] \tag{3.18}$$

- **Total power**

  Equation 3.19 defines the total power ($POWER$) which corresponds to the integrated area of the power spectrum [34].

$$POWER = \mu_0 \tag{3.19}$$

- **n% power frequency**

  The n% power frequency corresponds to the frequency below which n% of the total power is found. It is defined as $v\Delta f$, v being the smallest integer for which Equation 3.20 is satisfied. We selected the 50%, 85% and 95% power frequencies.

$$\sum_{m=3}^{v} G[m] \geq \frac{n\mu_0}{100} \tag{3.20}$$

- **Centroidal frequency**

  Equation 3.21 shows the expression of the centroidal frequency ($CFREQ$) which corresponds to the frequency at which the spectral mass is concentrated. It is defined as the square root of the ratio of the second to the zeroth spectral moments [34].

$$CFREQ = \sqrt{\frac{\mu_2}{\mu_0}} \tag{3.21}$$

- **Frequency dispersion**

  Equation 3.22 shows the expression of the frequency dispersion ($FREQD$), a unitless measure taking values between zero and one. It is worth zero for a pure sinusoid and increases with spectral bandwidth to a maximum of one. It is an indicator of the variability in the frequency content of the power spectral density [34].

$$FREQD = \sqrt{1 - \frac{\mu_1^2}{\mu_0 \mu_2}} \tag{3.22}$$

Computation of the peak frequency of the signal, i.e the frequency associated to the highest amplitude in the PSD, can also been found in the literature [8]. However, we decided not to include it in our study considering Baratto et al.[7] argue "[it] is not informative because it is related to the prevalent frequency of the signal, and this is determined by the biomechanics of sway rather than by the underlying cibernetics" [7].

3.4 Statistical analysis

We conducted a comprehensive statistical analysis in order to be able to quantitatively compare the results of the data processing pipeline for both the force plate and the Wii Balance Board. Various statistical procedures commonly used in the field were applied in order to find out if there were significant differences between the features estimated by the WBB and the FP. Since each of the 6 participants went through a single session of twelve trials (3 on each balance board), a total of 72 data points were available for our analysis. We decided to pool those results in our study to have more statistically significant results.

3.4.1 Data preparation

Before computing any statistics, we had to perform basic data cleaning. Out of the 72 acquisition files, two duplicate acquisitions were found and so we removed them. The reason behind the existence of such duplicates is unknown and probably is the result of some human error during data collection. We also decided to conduct an outlier detection study. Assuming a Gaussian distribution of the posturographic measurements, we can use the z-score , also known as the standard score[1], to identify outliers. Such metric indicates how many standard deviations a data point is from the sample's mean. We used a 4 standard deviation threshold to identify outliers. After having identified 3 distinct

[1] https://en.wikipedia.org/wiki/Standard_score

outliers through this method, we performed a visual inspection of the corresponding acquisition data COP time series to identify the cause of the anomalies. We concluded such outliers were due to experimental errors where the subject, for example, suddenly stood off and back on the measurement setup which resulted in erroneous measurements. For consistency of the results, the decision was made to remove such outliers from the statistical analysis as they are a source of meaningless bias. Finally and because no calibration procedure was used, we rescaled all the Wii Balance Board data to allow for a more fair comparison of the features.

3.4.2 Exploratory data analysis

In the first part of the statistical analysis, we pursued the goal of getting a better understanding as well as a global overview of the data. In order to do so, we generated extensive statistical reports for both the WBB and the FP data. For each feature, the following information was computed:

- **Essentials:** number of observations, number of variables, variable type (numeric, categorical, boolean, data, etc...), number of distinct values, % of missing values
- **Quantile statistics:** minimum value, 5-th percentile, Q1, median, Q3, 95-th percentile, maximum, range, interquartile range
- **Descriptive statistics:** standard deviation, coefficient of variation, kurtosis, mean, median absolute deviation (MAD), skewness, sum, variance
- **Most frequent and extreme values:** 10 most frequent values, 5 minimum and maximum values
- **Histogram**
- **Correlations:** Spearman and Pearson correlation matrices

3.4.3 Linear regressions

Assuming a linear relationship between the FP and the WBB feature computations results, a common way to assess the strength of the association between the two devices is to perform a linear regression study for each feature. Based on the observation that neither the FP nor the WBB are free from observational errors, we decided to use the total least squares (TLS) modeling technique. More specifically, we performed a orthogonal distance regression (ODR), which consists in minimizing the sum of squared perpendicular distances, also called true distances, from the data points to the regression line [37].

This method contrasts with the ordinary least squares regression which only takes into account the error of the observed variable by minimizing the sum of squared vertical distances as shown in Figure 3.3. Fundamentally, performing a principal component analysis (PCA[2]) and taking the first component results would yield the same results.

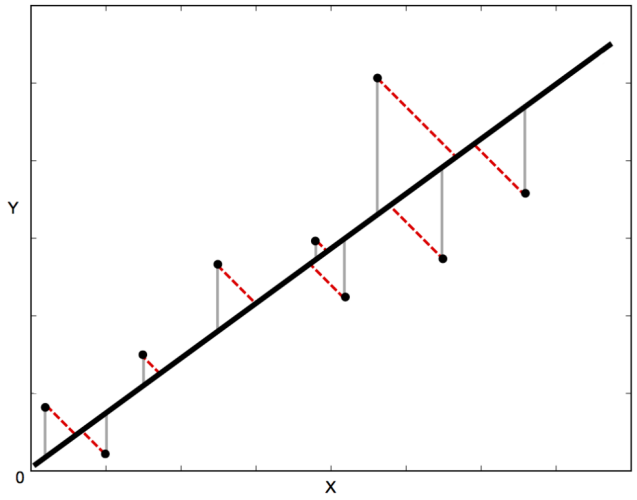

FIGURE 3.3: Least square residuals: total least squares (dotted red lines) versus ordinary least squares regression (grey lines).

3.4.4 Bland-Altman plots

Bland-Altman (BA) plots are designed to assess agreement between two measurements techniques, often a gold standard versus a new measurement device [38]. Figure 3.4 shows how such plots are constructed. The mean of the two measurements is plotted on the x axis and the difference between the two measurements on the y axis. The mean difference is added on top and represents the estimated bias. The 95% limits of agreement, or reference interval, defined as the mean difference ± 2 standard deviation of the difference, define upper and lower limits for the random fluctuations around the estimated bias[3]. Such graphs make it easy to identify any systematic difference between the measurements or possible outliers by a simple visual check or, alternatively, by performing a regression analysis. It is important to keep in mind that although useful for assessing agreement, "the best way to use the BA plot system would be to define a priori the limits of maximum acceptable differences (limits of agreement expected), based on biologically and analytically relevant criteria" [39]. To this day, such a priori limits haven't been identified yet.

[2] https://en.wikipedia.org/wiki/Principal_component_analysis
[3] https://en.wikipedia.org/wiki/Bland-Altman_plot

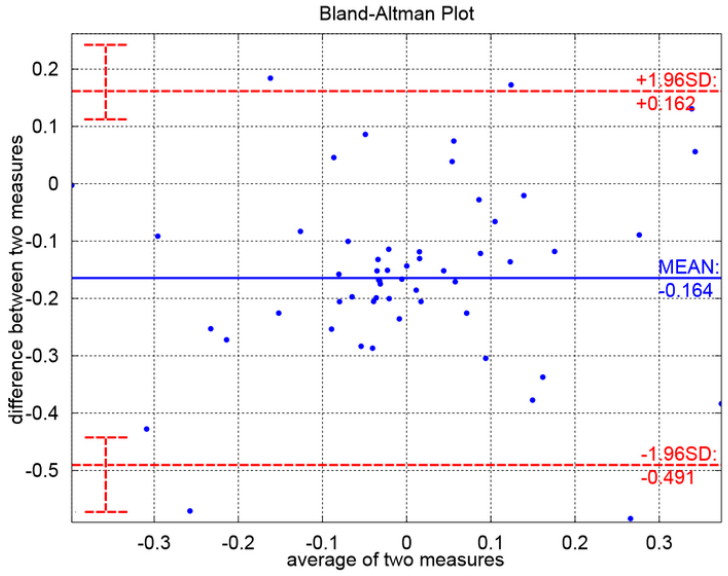

FIGURE 3.4: Structure of Bland-Altman plot.

3.4.5 Intraclass correlation coefficients

The intraclass correlation coefficient or ICC statistic can be used to assess the consistency of measurements between trials and devices. As such, it is a composite measure of intra-observer and inter-observer variability[4]. The approach followed by [25] consisted of computing the difference between the FP and the WBB measurements as a baseline for the ICC computations. Based on the 6 subjects performing 3 trials on each of the WBB, they defined 4 groups of 18 differences for each feature and computed the ICCs between those 4 groups. Following the ICC selection process flowchart from [40], we used a two-way random model, single rating, absolute agreement ICC(A,1) to perform an inter-rater (FP and WBB) reliability study. We pooled the results of the 4 Balance Board together as well as the corresponding FP results (using the mean of the three trials), leading to 24 distinct values (6 subjects and 4 balance boards) for each feature and device. The reader can refer to Table 3.2 for the most recent ICC interpretation guidelines [40].

ICC range	Inter-rater agreement quality
< 0.5	poor
$0.5 \leq \text{ICC} < 0.75$	moderate
$0.75 \leq \text{ICC} < 0.9$	good
$\text{ICC} \geq 0.9$	excellent

TABLE 3.2: ICC classification guidelines.

[4] https://en.wikipedia.org/wiki/Intraclass_correlation

Chapter 4

Results

Our experimental results are presented in this chapter. The first part of the chapter covers the results of the preprocessing pipeline while the second one is dedicated to the presentation of our statistical analysis results. We conclude the chapter with a critical discussion of our findings.

4.1 Center of pressure computations preliminary results

We detailed our preprocessing pipeline in section 3.2. For illustratory purposes, the following sections show some examples of the preprocessed COP time series and the associated power spectrums for both the WBB and the FP.

4.1.1 Stabilograms and statokinesigrams

Examples of the preprocessed COP displacement time series in the AP and ML directions as well as the resultant distance time series are represented on Figure 4.1. A rapid visual inspection of the graphs suggests there is a good correspondence between the FP and the WBB time series. Looking at the stabilograms, one can also observe that the COP amplitude is greater in the AP direction for both devices. This is verified on all the obtained stabilograms throughout the study. The statokinesigram, which corresponds to the excursions of the body in the horizontal plane, is also shown on Figure 4.1. The Wii Balance Board stabilograms and statokinesigram obtained with two different resampling methods are represented on Figure 4.2. The comparison of resampling algorithms on WBB COP data by Audifren and Contal [1] did not include the Fourier resampling method. We can see that using a Fourier resampling leads to additional noise and presence of plateaus in the stabilograms.

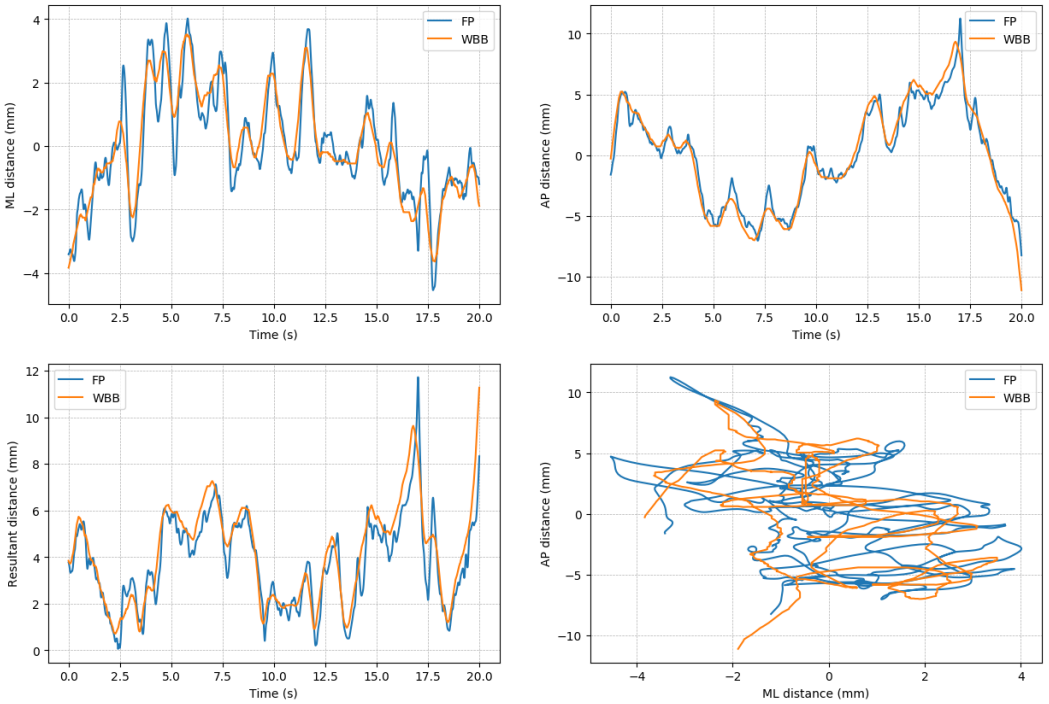

FIGURE 4.1: Superposition of Wii Balance Board and AMTI force plate stabilograms and statokinesigram. We used a time window length of $\Delta = 0.6$ s for the SWARII.

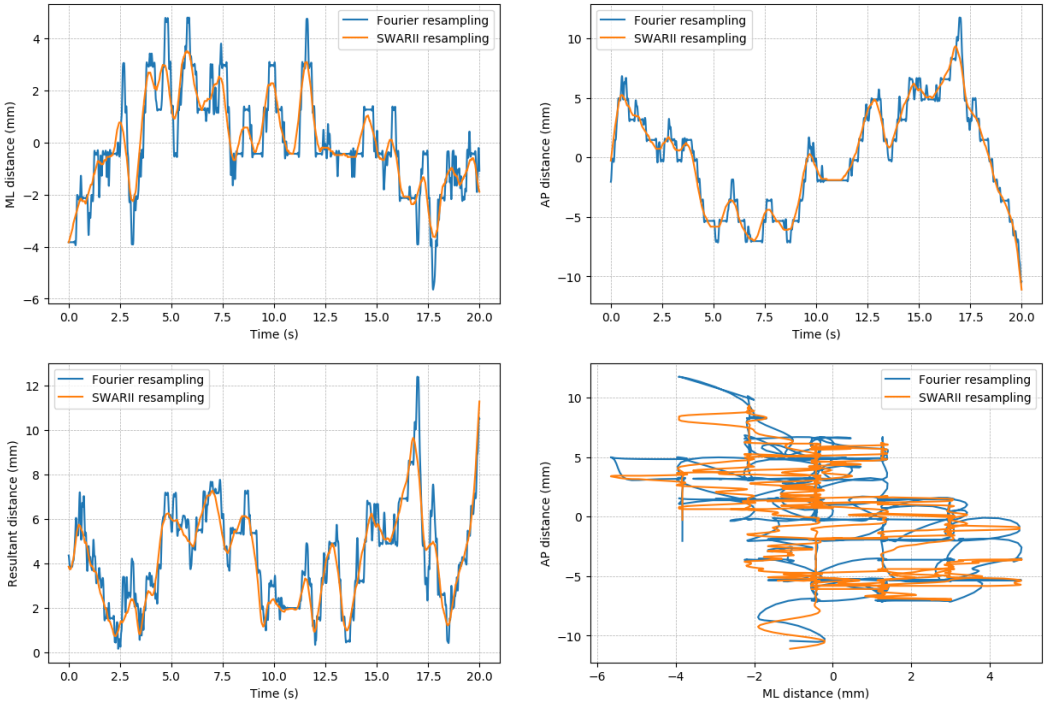

FIGURE 4.2: Example of Wii Balance Board stabilograms and statokinesigram using two different resampling schemes. We used a time window length of $\Delta = 0.6$ s for the SWARII.

One important point to keep in mind when using the SWARII algorithm is that we need to carefully tune the time window length parameter Δ as it controls the amount of smoothing of the estimation [1]. Figure 4.3 gives a visual representation of the effect of the choice of Δ on the outcome of the algorithm. Choosing a value too low will result in a highly noisy resampled signal while selecting a value too high leads to information loss.

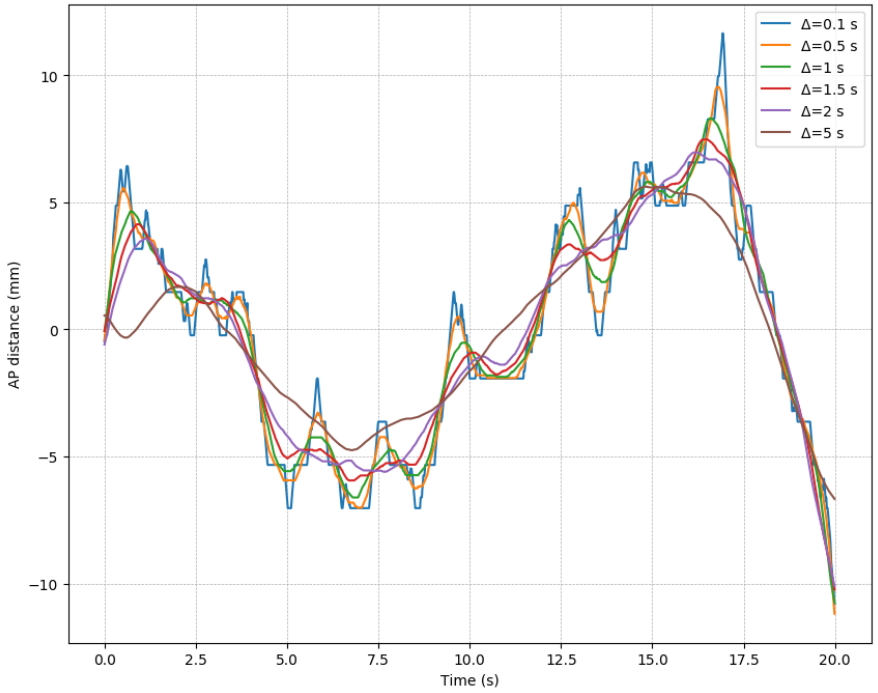

FIGURE 4.3: Influence of the SWARII time window length on the smoothness of the interpolation.

4.1.2 Power spectral density plots

Power spectral density plots obtained through the Fourier transformation of the preprocessed COP time series are shown on Figure 4.4 for both devices. A logarithmic scale is used on the y axis since the amplitude of the spectrum decreases exponentially as a result of the fact that most of the total power ($> 99\%$) is located in the low frequencies (< 10 Hz) [41]. Here again, inspection of the plots suggests there is a good correspondence between the FP and the WBB power spectral densities. Naturally, we observe higher amplitudes of the PSD in the anterior-posterior direction as we saw previously that the overall COP displacement is greater in this direction. We notice a slight deviation of the WBB PSD from the FP PSD in the higher frequencies but this is negligible considering the log scale used here.

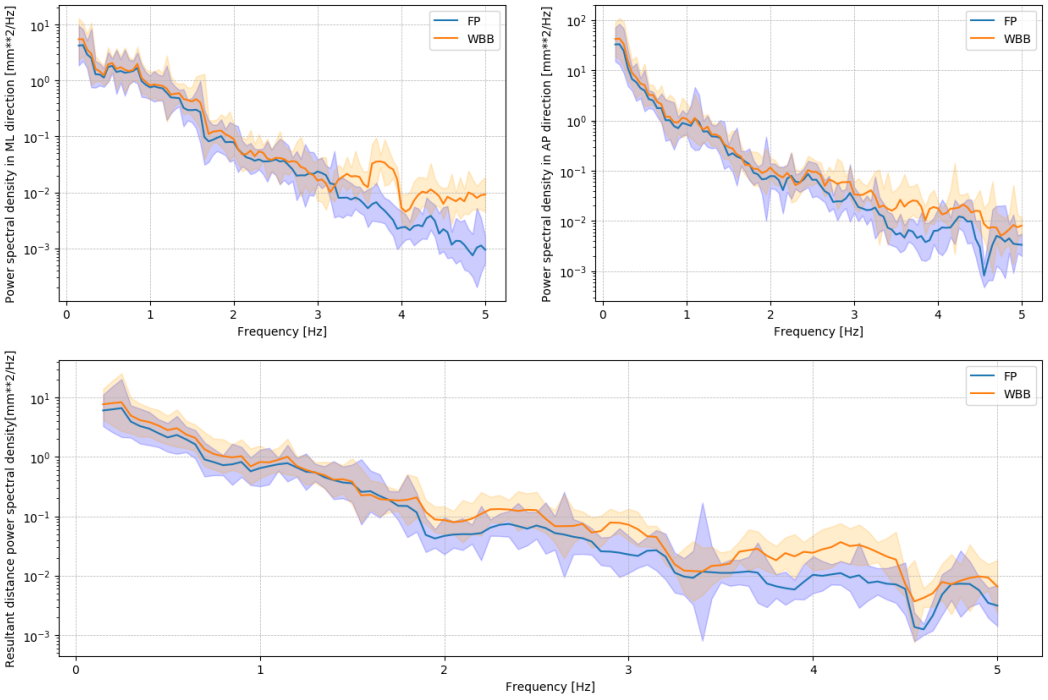

FIGURE 4.4: Superposition of Wii Balance Board and AMTI force plate power spectral density plots with 95% confidence intervals.

4.2 Statistical analysis results

4.2.1 Descriptive statistics

We mentioned in subsection 3.4.2 that we generated reports containing commonly used statistics. In order not to overload this chapter, we did not include most of those results except for the Pearson correlation matrices. However, the complete original results are available online in the form of dynamic reports.

The Pearson correlation matrices of the AMTI force plate and Wii Balance Board time and frequency domain features are shown on Figure 4.5 and Figure 4.6. Looking at the correlation heat maps, one can make multiple observations. First of all, both devices exhibit the same global patterns regarding features correlations. This is valid for features defined in both the time and frequency domains. Secondly, the time domain features seem to contain a lot of redundant information as there is a greater proportion of features that are highly correlated compared to frequency domain features. We previously defined three types of time domain features in subsection 3.3.2, namely the distance features, the area features and the hybrid features. We can see on Figure 4.5 that the distance and area features are highly positively correlated while both categories are highly negatively correlated to the hybrid features except for features related to COP velocity. One

hybrid feature, the mean frequency in the ML direction, shows little correlation to most of the other features. On the frequency domain side, it appears that the 50%, 85% and 95% power frequencies and the centroidal frequency (c.f subsubsection 3.3.3.2) are strongly correlated altogether except when comparing features defined in the ML and AP directions.

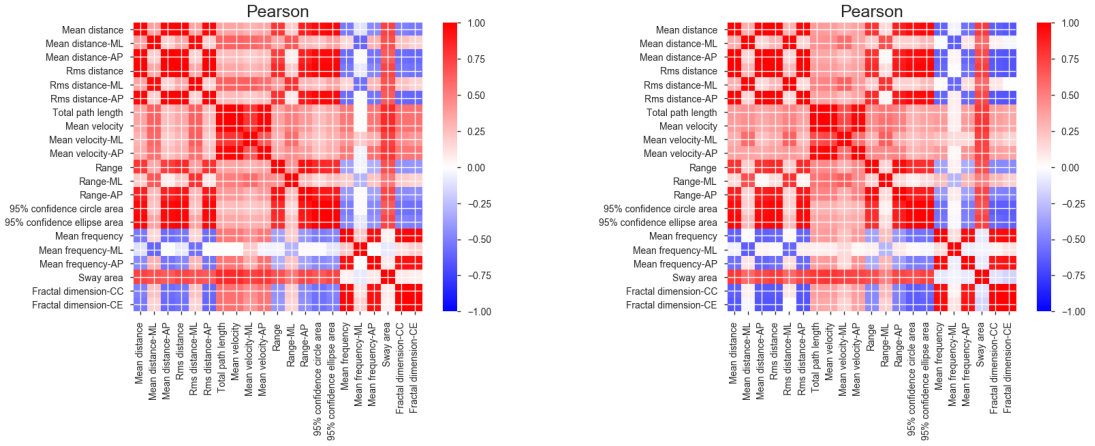

(A) AMTI force plate (B) Wii Balance Board

FIGURE 4.5: Time domain features Pearson correlations matrices.

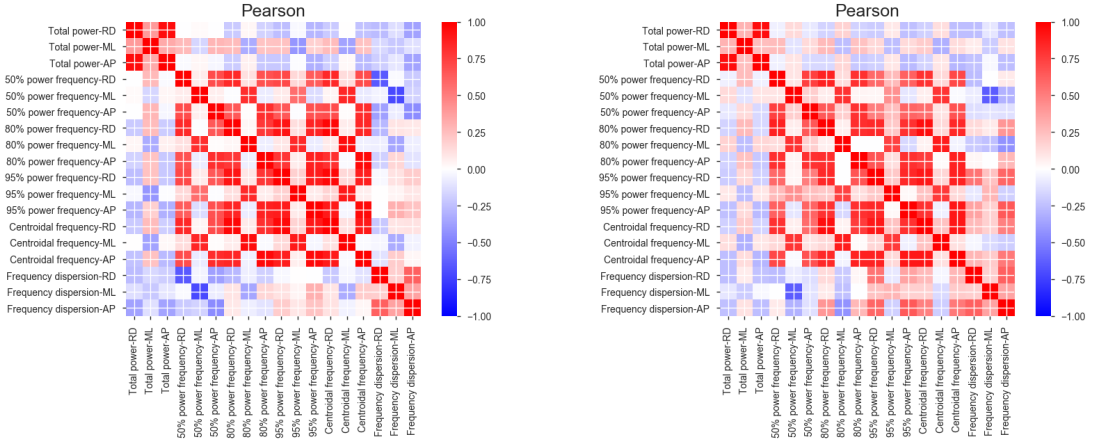

(A) AMTI force plate (B) Wii Balance Board

FIGURE 4.6: Frequency domain features Pearson correlations matrices.

4.2.2 Linear regressions

The orthogonal distance regressions results of the time and frequency domains features are presented on Figure 4.7 and Figure 4.8 respectively. Close inspection of the time domain results suggest there is a strong correspondence between the Wii Balance Board and the AMTI force plate measurements for most of the features. The distance and area features appear more strongly correlated than the hybrid features.

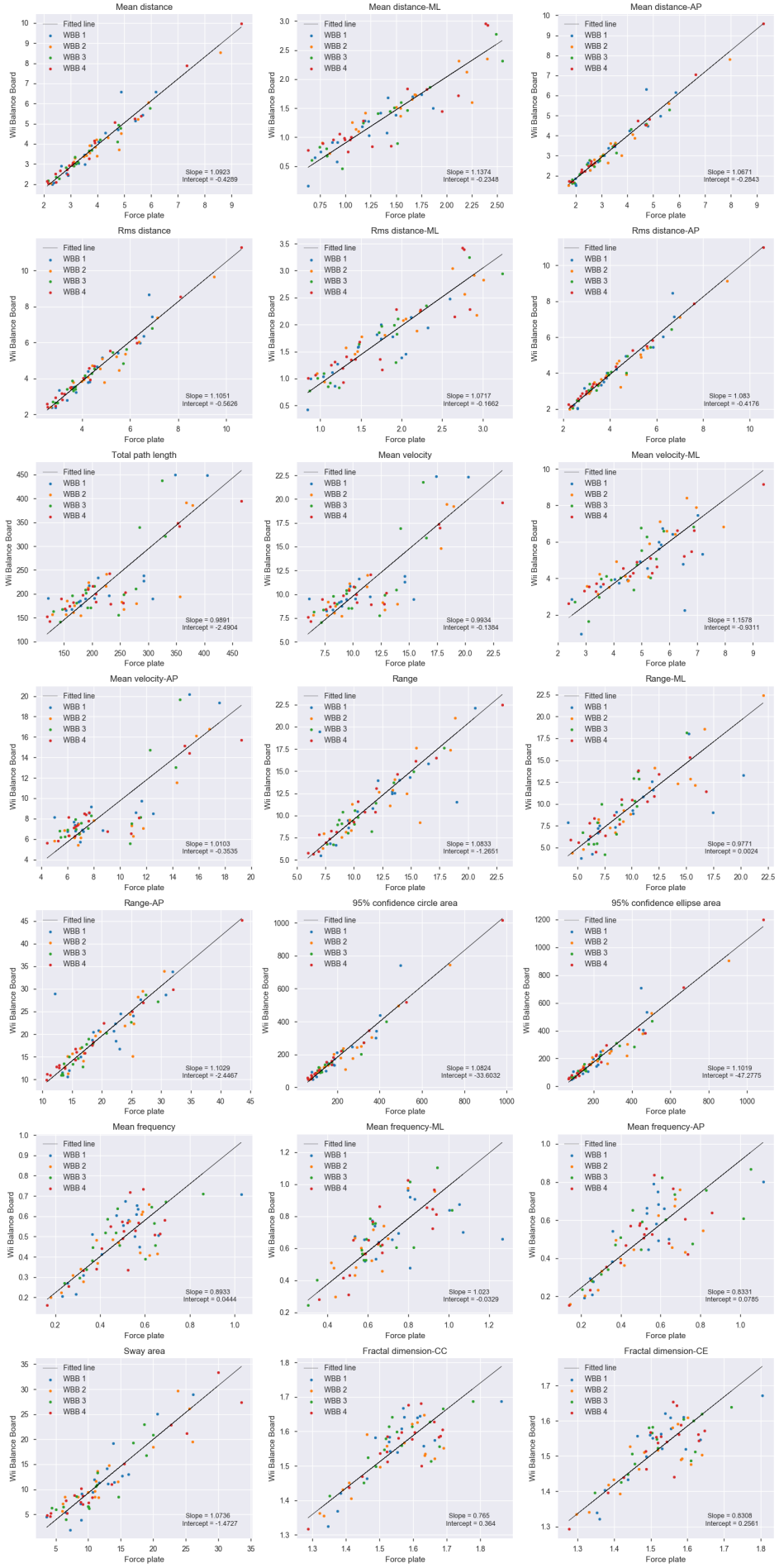

FIGURE 4.7: Orthogonal distance regressions results for the 21 time domain features.

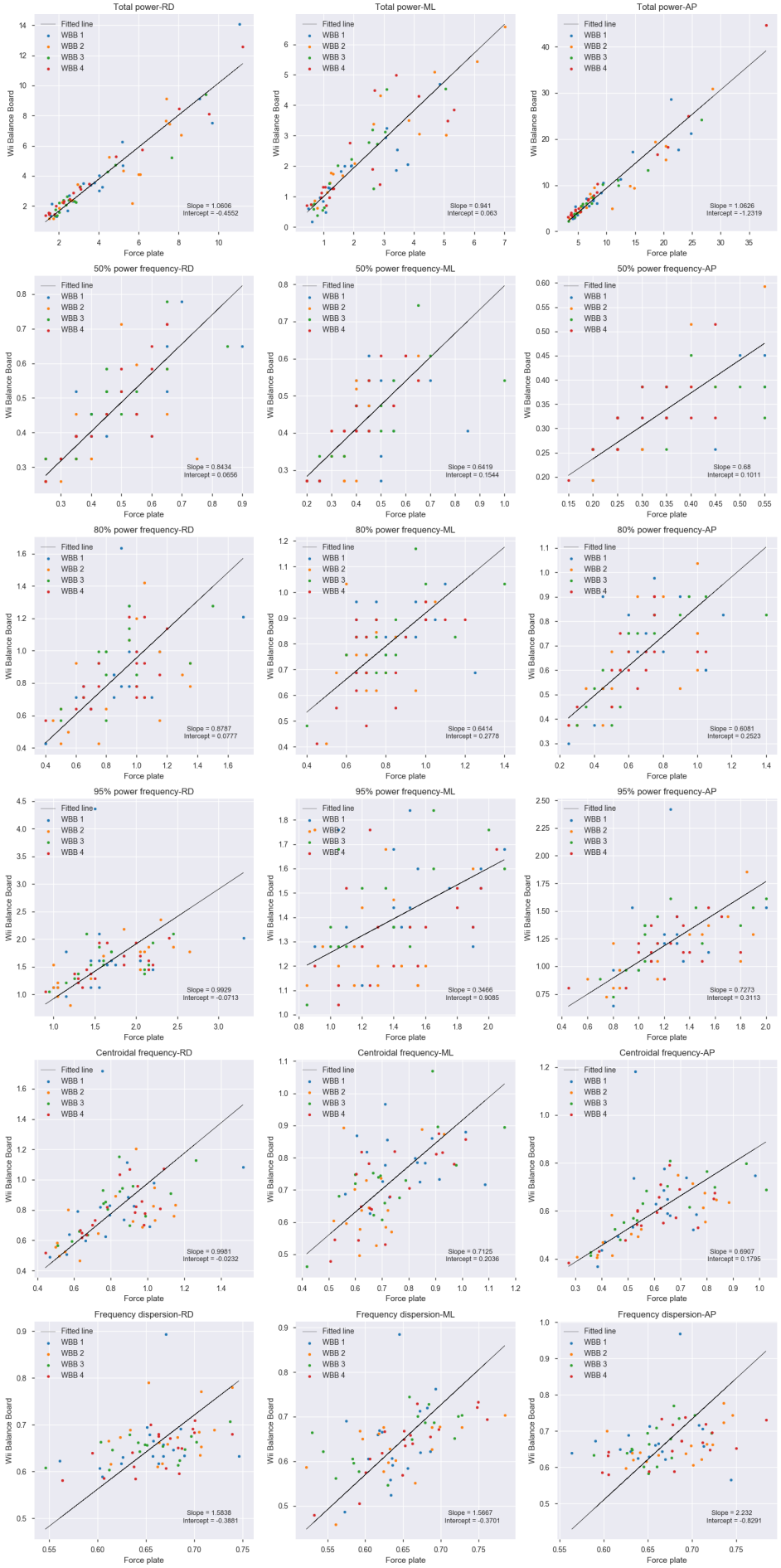

FIGURE 4.8: Orthogonal distance regressions results for the 18 frequency domain features.

However, one must pay great attention to the scales of the plots when comparing the results obtained for the different features as we can not directly quantify the quality of the fit in the case of the orthogonal distance regression.

The frequency domain results also show overall good correlations. The regression lines of the resultant distance frequency dispersion and the frequency dispersion in the AP direction are not very representative of the underlying correlation as they seem to be highly influenced by the presence of an outlier in the first WBB data.

4.2.3 Bland-Altman plots

Figure 4.9 and Figure 4.10 show the results of our Bland-Altman plots for both the time and frequency domains features. As per [39], 95% of the data points should be contained within the reference interval. Using a total of 72 observations and rounding to the nearest lower integer, we find that at least 68 observations should lie within the upper and lower limits of agreement in order to validate the agreement between the two devices. Out of the 21 features defined in the time domain, five of them do not satisfy this criterion and only two for the 18 frequency domain features. This means both devices agree on more than 76% of the time domain features and on more than 88% of the frequency domain features. Furthermore, we observe an estimated bias (average of the differences) close to zero on all plots but this is mostly a consequence of the WBB data rescaling. Inspection of the results also suggest no major proportional bias exists between the two methods since there is no noticeable trend between the variability of the differences and the mean difference for most of the features.

4.2.4 Intraclass correlation coefficients

The raw ICC time and frequency domains results are presented in Table 4.2 and Table 4.3 and summarized in Table 4.1 using the interpretation guidelines from Table 3.2. More than half of the time domain features showed excellent reliability and the remaining ones were evenly distributed between good and moderate reliability. All moderately reliable features belonged to the hybrid time domains features (mean frequencies and fractal dimensions).

	Excellent	Good	Moderate	Poor
Time domain features	11	5	5	0
Frequency domain features	3	3	10	2

TABLE 4.1: Intraclass correlation coefficients results distribution.

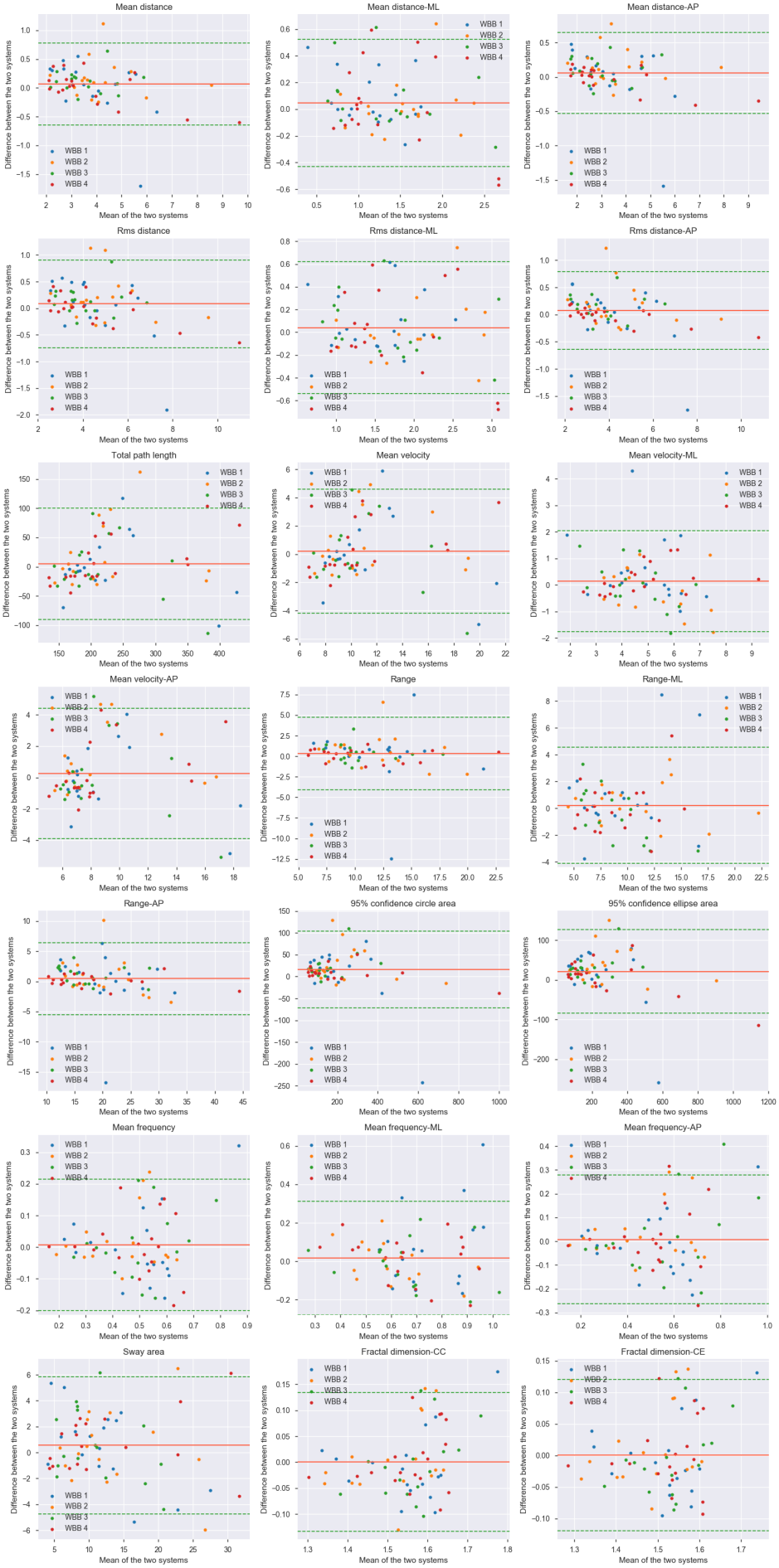

FIGURE 4.9: Bland-Altman plots for the 21 time domain features. Continuous red lines represent the mean difference between the devices. Dashed green lines indicate upper and lower limit of agreement (2 SD).

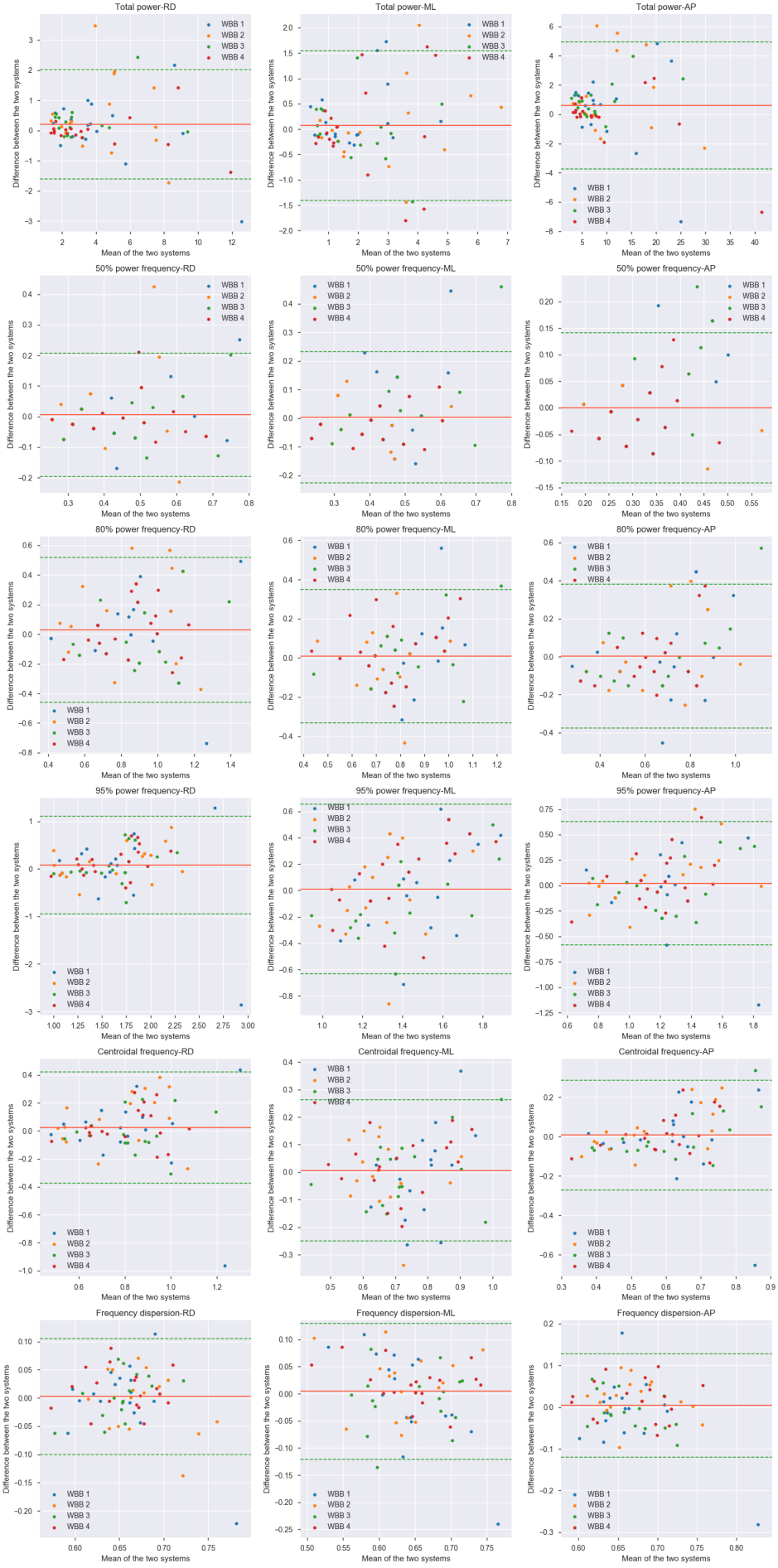

FIGURE 4.10: Bland-Altman plots for the 18 frequency domain features. Continuous red lines represent the mean difference between the devices. Dashed green lines indicate upper and lower limit of agreement (2 SD).

Feature	ICC(A,1)	95% CI	P-value
Mean distance	0.967	0.926 - 0.986	$1.27 \cdot 10^{-15}$
Mean distance-ML	0.932	0.849 - 0.97	$3.13 \cdot 10^{-12}$
Mean distance-AP	0.978	0.95 - 0.99	$1.33 \cdot 10^{-17}$
Rms distance	0.965	0.922 - 0.985	$2.17 \cdot 10^{-15}$
Rms distance-ML	0.946	0.88 - 0.976	$3.88 \cdot 10^{-13}$
Rms distance-AP	0.977	0.947 - 0.99	$2.09 \cdot 10^{-17}$
Total path length	0.867	0.721 - 0.94	$1.02 \cdot 10^{-8}$
Mean velocity	0.878	0.741 - 0.945	$4.22 \cdot 10^{-9}$
Mean velocity-ML	0.854	0.696 - 0.934	$2.75 \cdot 10^{-8}$
Mean velocity-AP	0.874	0.734 - 0.943	$5.85 \cdot 10^{-9}$
Range	0.86	0.707 - 0.937	$1.48 \cdot 10^{-8}$
Range-ML	0.946	0.88 - 0.976	$5.11 \cdot 10^{-13}$
Range-AP	0.924	0.835 - 0.966	$1.91 \cdot 10^{-11}$
95% confidence circle area	0.948	0.854 - 0.979	$2.42 \cdot 10^{-14}$
95% confidence ellipse area	0.945	0.834 - 0.978	$3.57 \cdot 10^{-14}$
Mean frequency	0.711	0.443 - 0.863	$3.41 \cdot 10^{-5}$
Mean frequency-ML	0.5	0.135 - 0.747	$5.47 \cdot 10^{-3}$
Mean frequency-AP	0.742	0.494 - 0.879	$1.11 \cdot 10^{-5}$
Sway area	0.951	0.892 - 0.978	$1.19 \cdot 10^{-13}$
Fractal dimension-CC	0.732	0.478 - 0.874	$1.6 \cdot 10^{-5}$
Fractal dimension-CE	0.731	0.477 - 0.873	$1.65 \cdot 10^{-5}$

TABLE 4.2: Intraclass correlation coefficients, 95% confidence intervals and P-values for the 21 time domain features using a single rating, absolute agreement, 2-way random effects model.

Feature	ICC(A,1)	95% CI	P-value
Total power-RD	0.962	0.906 - 0.984	$2.04 \cdot 10^{-15}$
Total power-ML	0.953	0.895 - 0.979	$1.07 \cdot 10^{-13}$
Total power-AP	0.956	0.896 - 0.981	$1.53 \cdot 10^{-14}$
50% power frequency-RD	0.81	0.613 - 0.912	$4.77 \cdot 10^{-7}$
50% power frequency-ML	0.53	0.175 - 0.764	$3.2 \cdot 10^{-3}$
50% power frequency-AP	0.761	0.527 - 0.889	$5.01 \cdot 10^{-6}$
80% power frequency-RD	0.598	0.271 - 0.803	$7.91 \cdot 10^{-4}$
80% power frequency-ML	0.52	0.161 - 0.758	$3.87 \cdot 10^{-3}$
80% power frequency-AP	0.754	0.514 - 0.885	$6.81 \cdot 10^{-6}$
95% power frequency-RD	0.451	0.075 - 0.717	$1.14 \cdot 10^{-2}$
95% power frequency-ML	0.42	0.034 - 0.698	$1.83 \cdot 10^{-2}$
95% power frequency-AP	0.638	0.329 - 0.824	$3.03 \cdot 10^{-4}$
Centroidal frequency-RD	0.593	0.264 - 0.8	$8.84 \cdot 10^{-4}$
Centroidal frequency-ML	0.553	0.207 - 0.778	$2.07 \cdot 10^{-3}$
Centroidal frequency-AP	0.654	0.354 - 0.833	$1.94 \cdot 10^{-4}$
Frequency dispersion-RD	0.637	0.328 - 0.824	$3.09 \cdot 10^{-4}$
Frequency dispersion-ML	0.66	0.363 - 0.836	$1.66 \cdot 10^{-4}$
Frequency dispersion-AP	0.576	0.238 - 0.79	$1.3 \cdot 10^{-3}$

TABLE 4.3: Intraclass correlation coefficients, 95% confidence intervals and P-values for the 18 frequency domain features using a single rating, absolute agreement, 2-way random effects model.

The frequency domain results were less convincing, showing moderate reliability for the majority of the features with the exception of total power related features demonstrating excellent reliability while the RD and ML 95% power frequencies showed poor reliability. Using a significance level of $\alpha = 0.05$ for the null hypothesis test, p-values show our results were all statistically significant.

4.3 Discussion

As described in section 3.1, we based our work on already existing data from prior research. Six subjects participated in the study. This is a rather low number compared to other similar studies which usually include around 20 participants. On the other hand, the total amount of acquisitions was still reasonable as each subject performed 3 trials on each of the 4 Wii Balance Boards. Moreover, the study was conducted on symptom free adults. This prevents us from drawing population specific conclusions regarding the usefulness of frequency domain measurements for balance assessment. It is also important to keep in mind that a static measurement protocol was used (still double limb standing condition) and, as such, our results are only relevant for postural steadiness assessment. Extra caution should be taken when expanding them to dynamic tasks.

An other important point is that the balance boards used in the previous study (and therefore in our study) had voluntarily not been calibrated. However, we saw in chapter 2 that using such linear calibration procedures can reduce the COP measurement error. Getting rid of the calibration step has little consequences when comparing WBB measurements between each of other but becomes problematic when comparing balance boards with calibrated force plates. One can rightfully ask oneself if such comparison is fair and will not yield inconsistent results. As a matter of fact, this had a considerable impact on our statistical analysis results and introduced a lot of bias in the Bland-Altman plots and ICCs computations. For this reason, we eventually decided to rescale the processed Wii Balance Board data to allow for a more accurate comparison.

Our approach to the signal processing also suffered from some caveats. First of all, as mentioned in section 3.2, we manually synchronized the two devices acquisition signals instead of adopting an automated and more robust approach. It is hard to quantify the impact it had on the quality of the results but we believe it is negligible considering the time lag was relatively small (< 0.5 second) compared to the studied time window (20 seconds) and consistent across measurements. Secondly, we decided to use the SWARII resampling scheme to palliate the effects of the variable sampling frequency of the WBB. To this day, the reasons behind this sampling jitter are not totally transparent and those

inconsistencies could be the result of data transmission problems linked to the usage of the Bluetooth protocol. We should also not ignore the fact that the WBB was designed as a low-cost gaming device and therefore is limited by the hardware quality and its inherent purpose. Nevertheless, it is very likely that directly collecting data from the WBB sensors through a wired connection to the device would allow to alleviate those discrepancies and remove the need for this custom resampling mechanism.

It is worth mentioning that even though we used the data from [25], our results are not directly comparable. The main reason for this is that our work was not focused on validating the interchangeability of the Wii Balance Board and, therefore, we computed our statistics differently by pooling the data of the four devices together. Looking at the literature (c.f chapter 2), we saw that most studies were computing a very limited set of time domain features when validating the WBB against force plates; the center of pressure total path length and velocity being the predominant ones. Less frequently, the 95% confidence ellipse area, COP ranges and root mean square distances in AP and ML direction were encountered. We only found one study that reported using hybrid time domain features such as the sway area [16]. To the best of our knowledge, neither the mean frequency and fractal dimension hybrid features nor the 95% confidence circle area feature have yet been validated on Wii Balance Boards. When it comes to previously validated features, our ICC and BA plots results are consistent with the literature, suggesting there is a good agreement between Wii Balance Boards and force plates balance measurements for healthy adults. While the Mean Frequency-ML had a significantly lower ICC than the rest of the features, the mean frequencies (RD and AP) and the fractal dimensions (CC and CE) ICCs showed moderate reliability. On the other hand, we also saw that those features are not very correlated to the distance and area measurements, suggesting they could capture additional information regarding postural steadiness. The 95% confidence circle area had a reliability score similar to the 95% circle area, both being excellent. They could therefore possibly be interchangeable. The sway area was the only hybrid feature demonstrating excellent reliability.

To this day, frequency domain features are simply absent from WBB validation studies found in the literature, preventing us from comparing our results to previous ones. Baratto et al.[7] analyzed the reliability and discriminative power of 38 parameters "in the general framework of a biomechanical model of postural stabilization" [7], including global frequency domain parameters. They shortlisted 4 particularly valuable parameters in which the 80% power frequency (also called the first frequency band (FB1) in their paper) was present. Having the WBB reliably measure this parameter would likely increase its balance assessment capabilities. In our study, ICC results for the 50% and 80% power frequencies went from moderate to good. Two of the 50% power frequencies and the 80% power frequency-AP had ICCs > 0.75. However, it is obvious that our study

suffered from a huge limitation which was the frequency resolution of the signal. With a 20 seconds acquisition duration (after preprocessing), the effective frequency resolution of the signal was 0.05 Hz. Unfortunately, very low frequencies account for a vast amount of the total power present in the PSD. It is clear by looking at the linear regressions and Bland-Altman plots that we would benefit from having a higher frequency resolution when computing the frequency domain features, especially the 50% and 80% power frequencies. The easiest and non artificial way to increase the frequency resolution is to increase the duration of the signal acquisition but this would probably not be very convenient neither realistic in the clinical practice. An alternative solution would be to perform a spectral interpolation of the signal using a time domain zero padding strategy which would yield a higher frequency resolution when switching to the frequency domain. On the other hand, the frequency resolution has no impact on the area under the PSD. As a consequence, features associated to the total power of the spectrum did not suffer from the relatively low frequency resolution. Nonetheless, the fact that excellent ICCs were obtained for those three features (> 0.95) is a very encouraging step towards a more fine-tuned validation study of the rest of the frequency domain features factoring in an appropriate granularity level of the frequency resolution.

It is also noteworthy to point out a few shortcomings of our statistical analysis. We used linear regressions to establish the presence of a linear relationship between the two devices measurements, implying they are measuring potentially well correlated variables. However Giavarina [39] claim that "two methods that are designed to measure the same variable should have good correlation when a set of samples are chosen in such manner that the property to be determined varies considerably" [39] and insists on the fact that good correlation does not imply good agreement. Regarding the Bland-Altman plots, we did not verify that the differences between the two systems were normally distributed as they should be in case of agreement. This could have been done visually using histograms plots or by means of a statistical test. We also omitted the confidence intervals for the 95% limits of agreement and the mean difference. Finally, we did not do any regression analysis on top of the BA plots to characterize the relationship between the variability of the differences and the mean difference.

Chapter 5

Future work and conclusion

We have extensively discussed some of the work that has already been done around comparative studies of the Wii Balance Board with force plates in chapter 2. To the best of our knowledge, none of them used any normalization methods when preprocessing the COP coordinates. De Oliveira [42] recently proposed a new method for stabilometric signals normalization which aims at reducing the intersubject and intrasubject variability in the scope of experiments including multiple conditions. Future studies could integrate this normalization procedure and investigate its impact on the WBB COP signal variability. Aside from signal normalization, there is room for improvement regarding other aspects of the signal processing. The SWARII algorithm used in our study offers a good trade-off between performance and ease of use as it requires tuning of only one parameter. According to the authors of the SWARII, there exists more complex resampling methods which could lead to better performances [1]. Despite them suggesting not to use such methods because deemed too complex, it is our belief they are still worth being investigated.

Although we covered a vast amount of time and frequency domain parameters, the scope of our validation study was still limited to what Baratto et al.[7] refers as "global posturographic parameters"[7]. Those parameters are rather intuitive in the sense that they are directly related to the "size" of the sway patterns [7]. However, COP data can also be described from a structural point of view. Parameters derived from sway density plots and stabilogram diffusion plots fall in this category [7] and are being increasingly used in balance assessment studies. Recent publications [16, 29] have used machine learning approaches to assess the ability of the WBB to discriminate between specific populations using both global and structural parameters. However, global frequency domain parameters remain absent from those studies. Considering the huge advancements recently made in the field of deep learning, further research should be conducted to see if the

most recent and state-of-the-art neural networks combined with advanced feature engineering and selection techniques can improve the classification performances reported up to now.

While our work was limited to postural steadiness, recent studies [43–46] have been trying to validate the device for the assessment and parametrization of COP displacement in dynamic scenarios. Having shown promising results so far, more work needs to be done to fully characterize the accuracy and precision of the WBB in dynamic transition tasks and derive suitable calibration techniques.

Another way of going past the limitations of the WBB would be to design and develop an alternative low-cost device targeting the clinical environment. Silva et al.[47] already discussed the design and development of such stabilometric apparatus. They claim their solution costs a tenth of commercial force platforms [47], which is still way above the WBB retail price. On the other hand, it is capable of measuring the vertical and horizontal components of the force as opposed to the WBB which is a uni-axial device. They also report a total uncertainty of the COP location smaller than 1 mm [47] which is closer to the 0.1 mm uncertainty recommended for posturography [21] than what the WBB can achieve, even with proper calibration. Perhaps further research could help decrease the price of this kind of application-specific hardware and provide a solid substitute to commercial force plates without compromising too much the quality of the measurements.

No matter the equipment used, there is no doubt low-cost posturography research would benefit from getting access to an open source software development kit for center of pressure based balance assessment. This would surely foster the interest of researchers and could help standardize the tools and methods used throughout the field, eventually bridging the gap between the expensive but trusted commercial force platforms and the much-needed low-cost devices.

Appendix A

Implementation

A.1 COP Features computations

```python
# Built-in modules imports
from utils import load_config

# Third-party module imports
import numpy as np
import json

config = load_config()


class CopFeatures:
    """
    Base class for COP based features computations.

    This class doesn't implement any feature computations and is simply responsible for parsing the COP data that will
    be used in COP based features computations in both the time and frequency domains.
    """

    acquisition_frequency = config["preprocessing_parameters"]["acquisition_frequency"]

    def __init__(self, cop_x, cop_y):
        self.cop_x = cop_x
        self.cop_y = cop_y
        self.cop_rd = self.compute_rd(self.cop_x, self.cop_y)
        self.N = self.cop_rd.size
        self.T = self.N / self.acquisition_frequency
```

```
27
28      @classmethod
29      def from_file(cls, filepath):
30          cop_x, cop_y = cls.parse_cop_data(filepath)
31
32          return cls(cop_x, cop_y)
33
34      @staticmethod
35      def parse_cop_data(filepath):
36          """Parse cop data from an input file."""
37
38          with open(filepath) as json_data:
39              cop_data = json.load(json_data)
40
41          cop_x = np.array(cop_data["COP_x"])
42          cop_y = np.array(cop_data["COP_y"])
43
44          return cop_x, cop_y
45
46      @staticmethod
47      def compute_rd(cop_x, cop_y):
48          """Compute the resultant distance vector from the x and y COP
        coordinates."""
49
50          return np.array([np.sqrt(x**2 + y**2) for x, y in zip(cop_x, cop_y)
        ])
```

A.2 Time domain features computations

```
1  # Built-in modules imports
2  from features import CopFeatures
3  from utils import load_config
4
5  # Third-party modules imports
6  import numpy as np
7  import warnings
8
9  config = load_config()
10
11
12 class DistanceFeatures(CopFeatures):
13     """
14     Class that implements the time domain distance features computations
       derived from the COP positions.
15     """
16
17     def __init__(self, cop_x, cop_y):
```

```
18          super(DistanceFeatures, self).__init__(cop_x, cop_y)
19          self.distance_features = self.compute_distance_features()
20
21      @staticmethod
22      def compute_mean_distance(array):
23          """Compute the mean value of an array using the numpy mean
    implementation."""
24
25          return array.mean()
26
27      def compute_rd_mean_distance(self):
28          """Compute the average distance from the mean COP."""
29
30          return self.compute_mean_distance(self.cop_rd)
31
32      def compute_ml_mean_distance(self):
33          """Compute the average ML distance from the mean COP."""
34
35          return self.compute_mean_distance(np.absolute(self.cop_x))
36
37      def compute_ap_mean_distance(self):
38          """Compute the average AP distance from the mean COP."""
39
40          return self.compute_mean_distance(np.absolute(self.cop_y))
41
42      @staticmethod
43      def compute_rms_distance(array):
44          """
45          Compute the root mean square value of an array using the numpy mean
    , root and square implementations.
46          """
47
48          rms_distance = np.sqrt(np.mean(np.square(array)))
49          return rms_distance
50
51      def compute_rd_rms_distance(self):
52          """Compute the root mean square distance from the mean COP."""
53
54          return self.compute_rms_distance(self.cop_rd)
55
56      def compute_ml_rms_distance(self):
57          """Compute the root mean square ML distance from the mean COP."""
58
59          return self.compute_rms_distance(self.cop_x)
60
61      def compute_ap_rms_distance(self):
62          """Compute the root mean square AP distance from the mean COP."""
63
```

```
64          return self.compute_rms_distance(self.cop_y)
65
66      @staticmethod
67      def compute_path_length(array1, array2):
68          distances_1 = np.diff(array1, axis=0)
69          distances_2 = np.diff(array2, axis=0)
70          path_length = np.sqrt((distances_1 ** 2) + (distances_2**2)).sum()
71
72          return path_length
73
74      def compute_rd_path_length(self):
75          """Compute the total length of the COP path."""
76
77          return self.compute_path_length(self.cop_x, self.cop_y)
78
79      def compute_ml_path_length(self):
80          """Compute the total length of the COP path in the ML direction."""
81
82          distances = np.absolute(np.diff(self.cop_x, axis=0))
83          path_length = distances.sum()
84
85          return path_length
86
87      def compute_ap_path_length(self):
88          """Compute the total length of the COP path in the AP direction."""
89
90          distances = np.absolute(np.diff(self.cop_y, axis=0))
91          path_length = distances.sum()
92
93          return path_length
94
95      def compute_rd_mean_velocity(self):
96          """Compute the average velocity of the COP."""
97
98          mean_velocity = (self.compute_rd_path_length()) / \
99              (self.cop_rd.size / self.acquisition_frequency)
100         return mean_velocity
101
102     def compute_ml_mean_velocity(self):
103         """Compute the average velocity of the COP in the ML direction."""
104
105         mean_velocity = (self.compute_ml_path_length()) / \
106             (self.cop_x.size / self.acquisition_frequency)
107         return mean_velocity
108
109     def compute_ap_mean_velocity(self):
110         """Compute the average velocity of the COP in the AP direction."""
111
```

```
112         mean_velocity = (self.compute_ap_path_length()) / \
113             (self.cop_y.size / self.acquisition_frequency)
114         return mean_velocity
115 
116     @staticmethod
117     def compute_range(min_value, max_value):
118         """Compute the range."""
119 
120         return np.absolute(min_value - max_value)
121 
122     def compute_rd_range(self):
123         """Compute the range of the resultant distance time series."""
124 
125         return self.compute_range(self.cop_rd.min(), self.cop_rd.max())
126 
127     def compute_ml_range(self):
128         """Compute the range in the ML direction."""
129 
130         return self.compute_range(self.cop_x.min(), self.cop_x.max())
131 
132     def compute_ap_range(self):
133         """Compute the range in the AP direction."""
134 
135         return self.compute_range(self.cop_y.min(), self.cop_y.max())
136 
137     def compute_sway_displacement(self):
138         return self.cop_rd.sum()
139 
140     def compute_distance_features(self):
141         """Compute all the distance features and store them in a dictionary
    ."""
142 
143         features = {}
144         features["Mean distance"] = self.compute_rd_mean_distance()
145         features["Mean distance-ML"] = self.compute_ml_mean_distance()
146         features["Mean distance-AP"] = self.compute_ap_mean_distance()
147         features["Rms distance"] = self.compute_rd_rms_distance()
148         features["Rms distance-ML"] = self.compute_ml_rms_distance()
149         features["Rms distance-AP"] = self.compute_ap_rms_distance()
150         features["Total path length"] = self.compute_rd_path_length()
151         features["Mean velocity"] = self.compute_rd_mean_velocity()
152         features["Mean velocity-ML"] = self.compute_ml_mean_velocity()
153         features["Mean velocity-AP"] = self.compute_ap_mean_velocity()
154         features["Range"] = self.compute_rd_range()
155         features["Range-ML"] = self.compute_ml_range()
156         features["Range-AP"] = self.compute_ap_range()
157 
158         return features
```

```
159
160     def summary(self):
161         """Print out a summary of the distance features to standard output.
        """
162
163         for key, value in self.distance_features.items():
164             print("{}: {}".format(key, value))
165
166
167 class AreaFeatures(DistanceFeatures):
168     """
169     Class that implements the time domain area features computations
        derived from the COP positions.
170     """
171
172     # Constants
173     z_05 = config["time_features_parameters"]["z_05"]
174     F_05 = config["time_features_parameters"]["F_05"]
175
176     def __init__(self, cop_x, cop_y):
177         super(AreaFeatures, self).__init__(cop_x, cop_y)
178         self.area_features = self.compute_area_features()
179
180     def compute_std_rd(self):
181         """Compute the standard deviation of the resultant distance time
        series."""
182
183         std_rd = np.sqrt(np.square(self.distance_features["Rms distance"])
        - np.square(
184             self.distance_features["Mean distance"]))
185         return std_rd
186
187     def compute_std_ml(self):
188         """Compute the standard deviation of the ML time series."""
189
190         return self.distance_features["Rms distance-ML"]
191
192     def compute_std_ap(self):
193         """Compute the standard deviation of the AP time series."""
194
195         return self.distance_features["Rms distance-AP"]
196
197     def compute_confidence_circle_area(self):
198         """Compute the 95% confidence circle area (AREA-CC)."""
199
200         std_rd = self.compute_std_rd()
201         area_cc = np.pi * \
202             np.square(
```

```
203                 self.distance_features["Mean distance"] + self.z_05 *
    std_rd)
204
205         return area_cc
206
207     def compute_confidence_ellipse_area(self):
208         """Compute the 95% confidence elipse area (AREA-CE)."""
209
210         std_ml = self.compute_std_ml()
211         std_ap = self.compute_std_ap()
212         area_ce = np.pi * self.F_05 * np.sqrt(np.square(np.square(std_ml))
    + np.square(np.square(std_ap)) + 6 * np.square(std_ml) * np.square(
    std_ap) -
213                                               4 * np.square(np.cov(self.
    cop_x, self.cop_y)[0][1]) - (np.square(std_ml) + np.square(std_ap)))
214
215         return area_ce
216
217     def compute_area_features(self):
218         """Compute all the area features and store them in a dictionary."""
219
220         features = {}
221         features["95% confidence circle area"] = self.
    compute_confidence_circle_area()
222         features["95% confidence ellipse area"] = self.
    compute_confidence_ellipse_area()
223
224         return features
225
226     def summary(self):
227         """Print out a summary of the area features to standard output."""
228
229         for key, value in self.area_features.items():
230             print("{}: {}".format(key, value))
231
232
233 class HybridFeatures(AreaFeatures):
234     """
235     Class that implements the time domain hybrid features computations
    derived from the COP positions.
236     """
237
238     def __init__(self, cop_x, cop_y):
239         super(HybridFeatures, self).__init__(cop_x, cop_y)
240         self.hybrid_features = self.compute_hybrid_features()
241
242     def compute_sway_area(self):
243         """Compute the sway area."""
```

```
244
245         sway_values = []
246         T = (self.cop_rd.size / self.acquisition_frequency)
247         for i in range(len(self.cop_rd) - 1):
248             sway_values.append(np.absolute(
249                 self.cop_x[i + 1] * self.cop_y[i] - self.cop_x[i] * self.
    cop_y[i + 1]) / (2 * T))
250
251         sway_area = np.array(sway_values).sum()
252
253         return sway_area
254
255     def compute_mean_frequency(self):
256         """Compute the mean frequency."""
257
258         mean_frequency = (self.distance_features["Mean velocity"]) / (
259             2 * np.pi * self.distance_features["Mean distance"])
260
261         return mean_frequency
262
263     def compute_mean_frequency_ml(self):
264         """Compute the mean frequency in the ML direction."""
265
266         mean_frequency_ml = (self.distance_features["Mean velocity-ML"]) /
    (
267             4 * np.sqrt(2) * self.distance_features["Mean distance-ML"])
268
269         return mean_frequency_ml
270
271     def compute_mean_frequency_ap(self):
272         """Compute the mean frequency in the AP direction."""
273
274         mean_frequency_ap = (self.distance_features["Mean velocity-AP"]) /
    (
275             4 * np.sqrt(2) * self.distance_features["Mean distance-AP"])
276
277         return mean_frequency_ap
278
279     def compute_fractal_dimension(self, d):
280         """Compute the fractal dimension (FD)."""
281
282         totex = self.compute_rd_path_length()
283         N = self.cop_rd.size
284         FD = (np.log(N)) / \
285             (np.log((N * d) / (totex)))
286
287         return FD
288
```

```
289     def compute_fractal_dimension_cc(self):
290         """Compute the fractal dimension-CC."""
291 
292         std_rd = self.compute_std_rd()
293         d_fd_cc = 2 * (self.distance_features["Mean distance"] + self.z_05
    * std_rd)
294 
295         return self.compute_fractal_dimension(d_fd_cc)
296 
297     def compute_fractal_dimension_ce(self):
298         """Compute the fractal dimension-CE."""
299 
300         std_ml = self.compute_std_ml()
301         std_ap = self.compute_std_ap()
302         d_fd_ce = np.sqrt(4 * self.F_05 * np.sqrt(np.square(np.square(
    std_ml))
303                                                   + np.square(np.square(
    std_ap))
304                                                   + 6 * np.square(std_ml) *
     np.square(std_ap)
305                                                   - 4 * np.square(np.cov(
    self.cop_x, self.cop_y)[0][1])
306                                                   - (np.square(std_ml) + np
    .square(std_ap))))
307 
308         return self.compute_fractal_dimension(d_fd_ce)
309 
310     def compute_hybrid_features(self):
311         """Compute all the hybrid features and store them in a dictionary.
    """
312 
313         features = {}
314         features["Mean frequency"] = self.compute_mean_frequency()
315         features["Mean frequency-ML"] = self.compute_mean_frequency_ml()
316         features["Mean frequency-AP"] = self.compute_mean_frequency_ap()
317         features["Sway area"] = self.compute_sway_area()
318         features["Fractal dimension-CC"] = self.
    compute_fractal_dimension_cc()
319         features["Fractal dimension-CE"] = self.
    compute_fractal_dimension_ce()
320 
321         return features
322 
323     def summary(self):
324         """Print out a summary of the hybrid features to standard output.
    """
325 
326         for key, value in self.hybrid_features.items():
```

```
            print("{}: {}".format(key, value))


class TimeFeatures(HybridFeatures):
    """
    Class that computes and merges all the time domain features.
    """

    def __init__(self, cop_x, cop_y):
        super(TimeFeatures, self).__init__(cop_x, cop_y)
        self.time_features = self.merge_time_features()

    def merge_time_features(self):
        """Merge all the time domain features together."""

        return {**self.distance_features, **self.area_features, **self.
    hybrid_features}

    def summary(self):
        """Print out a summary of the time features to standard output."""

        for key, value in self.time_features.items():
            print("{}: {}".format(key, value))
```

A.3 Frequency domain features computations

```
# Built-in modules imports
from features import CopFeatures
from utils import load_config
from mtspec import mtspec

# Third-party module imports
from scipy.signal import welch
from scipy.integrate import cumtrapz
import numpy as np

config = load_config()


class FrequencyFeatures(CopFeatures):
    """Class that implements the frequency domain features derived from the
    COP positions."""

    psd_method_used = config["frequency_features_parameters"]["psd_method"]
    fs = config["frequency_features_parameters"]["sampling_frequency"]
    frequency_range = config["frequency_features_parameters"]["
    frequency_range"]
```

```
20
21      # Welch periodogram parameters
22      nperseg = config["frequency_features_parameters"]["welch"]["nperseg"]
23
24      # Adaptive weighted multitaper spectrum parameters
25      delta = config["frequency_features_parameters"]["multitaper"]["delta"]
26      time_bandwidth = config["frequency_features_parameters"]["multitaper"][
        "time_bandwidth"]
27      number_of_tapers = config["frequency_features_parameters"]["multitaper"
        ]["number_of_tapers"]
28
29      def __init__(self, cop_x, cop_y):
30          super(FrequencyFeatures, self).__init__(cop_x, cop_y)
31
32          self.psd_methods_dict = self.create_psd_methods_dict()
33          default_psd = "multitaper"
34          self.psd_method_impl = self.psd_methods_dict.get(self.
        psd_method_used, self.psd_methods_dict[default_psd])
35
36          self.rd_spectral_density = self.psd_method_impl(self.cop_rd)
37          self.ml_spectral_density = self.psd_method_impl(self.cop_x)
38          self.ap_spectral_density = self.psd_method_impl(self.cop_y)
39          self.frequency_features = self.compute_frequency_features()
40
41      def create_psd_methods_dict(self):
42          psd_methods = {}
43          psd_methods["welch"] = self.compute_welch_psd
44          psd_methods["multitaper"] = self.compute_multitaper_psd
45
46          return psd_methods
47
48      def compute_multitaper_psd(self, array):
49          """
50          Estimate the adaptive weighted multitaper spectrum, as in Thomson
        1982. This is done by estimating the DPSS
51          (discrete prolate spheroidal sequences), multiplying each of the
        tapers with the data series, take the FFT,
52          and using the adaptive scheme for a better estimation. It outputs
        the power spectral density (PSD).
53
54          References
55          ----------
56            ..[1] mtspec package documentation: http://krischer.github.io/
        mtspec/multitaper_mtspec.html
57          """
58
59          psd, f = mtspec(data=array, delta=self.delta, time_bandwidth=self.
        time_bandwidth, number_of_tapers=self.number_of_tapers)
```

```
60          psd = psd[self.frequency_range[0]: self.frequency_range[1]]
61          f = f[self.frequency_range[0]: self.frequency_range[1]]
62
63          return (f, psd)
64
65      def compute_welch_psd(self, array):
66          """
67          Compute the power spectral density using the scipy implementation
    of the Welch method.
68
69          References
70          ----------
71           ..[1] Scipy documentation: https://docs.scipy.org/doc/scipy/
    reference/generated/scipy.signal.welch.html#scipy.signal.welch
72          """
73
74          nfft = len(array)
75          (f, psd) = welch(array, fs=self.fs, nperseg=self.nperseg, nfft=nfft
    )
76          psd = psd[self.frequency_range[0]: self.frequency_range[1]]
77          f = f[self.frequency_range[0]: self.frequency_range[1]]
78
79          return (f, psd)
80
81      @staticmethod
82      def compute_power_spectral_density_area(power_spectrum):
83          """
84          Compute the power spectral density cumulative area.
85
86          The cumulative integrated area is computed using the composite
    trapezoidal rule.
87          Scipy documentation: https://docs.scipy.org/doc/scipy/reference/
    generated/scipy.integrate.cumtrapz.html
88          """
89
90          (f, psd) = power_spectrum
91          return cumtrapz(psd, f)
92
93      def compute_rd_power_spectral_density_area(self):
94          """Compute the resultant distance displacement power spectral
    density cumulative area."""
95
96          return self.compute_power_spectral_density_area(self.
    rd_spectral_density)
97
98      def compute_ml_power_spectral_density_area(self):
99          """Compute the power spectral density area of the COP displacement
    in the ML direction."""
```

```
100
101         return self.compute_power_spectral_density_area(self.
    ml_spectral_density)
102
103     def compute_ap_power_spectral_density_area(self):
104         """Compute the power spectral density area of the COP displacement
    in the AP direction."""
105
106         return self.compute_power_spectral_density_area(self.
    ap_spectral_density)
107
108     def compute_rd_total_power(self):
109         """Compute the power spectral density total power."""
110
111         area = self.compute_rd_power_spectral_density_area()
112
113         return area[-1]
114
115     def compute_ml_total_power(self):
116         """Compute the total power in the ML direction."""
117
118         area = self.compute_ml_power_spectral_density_area()
119
120         return area[-1]
121
122     def compute_ap_total_power(self):
123         """Compute the total power in the AP direction."""
124
125         area = self.compute_ap_power_spectral_density_area()
126
127         return area[-1]
128
129     @staticmethod
130     def compute_peak_frequency(power_spectrum):
131         """Compute the peak frequency."""
132
133         (f, psd) = power_spectrum
134         p_max_index = psd.argmax()
135         f_peak = f[p_max_index]
136
137         return f_peak
138
139     def compute_rd_f_peak(self):
140         """Compute the resultant distance power spectral density peak
    frequency."""
141
142         return self.compute_peak_frequency(self.rd_spectral_density)
143
```

```
144     def compute_ml_f_peak(self):
145         """Compute the peak frequency in the ML direction."""
146 
147         return self.compute_peak_frequency(self.ml_spectral_density)
148 
149     def compute_ap_f_peak(self):
150         """Compute the peak frequency in the AP direction."""
151 
152         return self.compute_peak_frequency(self.ap_spectral_density)
153 
154     @staticmethod
155     def compute_power_frequency(n, power_spectrum_area, power_spectrum):
156         """Compute the n% power frequency.
157 
158         The n% power frequency is the frequency below which n% of the total
     power is found.
159         """
160 
161         (f, psd) = power_spectrum
162         threshold = (n / 100)
163         f_power_index = np.where(power_spectrum_area >= (threshold *
    power_spectrum_area[-1]))
164         f_power = f[f_power_index[0][0]]
165 
166         return f_power
167 
168     def compute_rd_power_frequency(self, n):
169         """Compute the resultant distance power spectral density n% power
    frequency."""
170 
171         power_spectrum_area = self.compute_rd_power_spectral_density_area()
172         (f, psd) = self.rd_spectral_density
173 
174         return self.compute_power_frequency(n, power_spectrum_area, (f, psd
    ))
175 
176     def compute_ml_power_frequency(self, n):
177         """Compute the n% power frequency in the ML direction."""
178 
179         power_spectrum_area = self.compute_ml_power_spectral_density_area()
180         (f, psd) = self.ml_spectral_density
181 
182         return self.compute_power_frequency(n, power_spectrum_area, (f, psd
    ))
183 
184     def compute_ap_power_frequency(self, n):
185         """Compute the n% power frequency in the AP direction."""
186 
```

```
187         power_spectrum_area = self.compute_ap_power_spectral_density_area()
188         (f, psd) = self.ap_spectral_density
189 
190         return self.compute_power_frequency(n, power_spectrum_area, (f, psd
    ))
191 
192     def compute_spectral_moment(self, k, psd_estimate):
193         delta_f = 5 * self.delta
194         spectral_moment = sum(
195             [np.power(((m + self.frequency_range[0]) * delta_f), k) * psd
    for m, psd in enumerate(psd_estimate)])
196 
197         return spectral_moment
198 
199     @staticmethod
200     def compute_centroidal_frequency(mu_0, mu_2):
201         """Compute the centroidal frequency."""
202 
203         return np.sqrt(mu_2 / mu_0)
204 
205     def compute_rd_centroidal_frequency(self):
206         """Compute the resultant distance power spectral density centroidal
     frequency."""
207 
208         mu_0 = self.compute_spectral_moment(0, self.rd_spectral_density[1])
209         mu_2 = self.compute_spectral_moment(2, self.rd_spectral_density[1])
210 
211         return self.compute_centroidal_frequency(mu_0, mu_2)
212 
213     def compute_ml_centroidal_frequency(self):
214         """Compute the resultant distance power spectral density centroidal
     frequency."""
215 
216         mu_0 = self.compute_spectral_moment(0, self.ml_spectral_density[1])
217         mu_2 = self.compute_spectral_moment(2, self.ml_spectral_density[1])
218 
219         return self.compute_centroidal_frequency(mu_0, mu_2)
220 
221     def compute_ap_centroidal_frequency(self):
222         """Compute the resultant distance power spectral density centroidal
     frequency."""
223 
224         mu_0 = self.compute_spectral_moment(0, self.ap_spectral_density[1])
225         mu_2 = self.compute_spectral_moment(2, self.ap_spectral_density[1])
226 
227         return self.compute_centroidal_frequency(mu_0, mu_2)
228 
229     @staticmethod
```

```
230     def compute_frequency_dispersion(mu_0, mu_1, mu_2):
231         """Compute the frequency dispersion."""
232         return np.sqrt(1 - (np.square(mu_1)) / (mu_0 * mu_2))
233 
234     def compute_rd_frequency_dispersion(self):
235         """Compute the resultant distance power spectral density centroidal
        frequency."""
236 
237         mu_0 = self.compute_spectral_moment(0, self.rd_spectral_density[1])
238         mu_1 = self.compute_spectral_moment(1, self.rd_spectral_density[1])
239         mu_2 = self.compute_spectral_moment(2, self.rd_spectral_density[1])
240 
241         return self.compute_frequency_dispersion(mu_0, mu_1, mu_2)
242 
243     def compute_ml_frequency_dispersion(self):
244         """Compute the resultant distance power spectral density centroidal
        frequency."""
245 
246         mu_0 = self.compute_spectral_moment(0, self.ml_spectral_density[1])
247         mu_1 = self.compute_spectral_moment(1, self.ml_spectral_density[1])
248         mu_2 = self.compute_spectral_moment(2, self.ml_spectral_density[1])
249 
250         return self.compute_frequency_dispersion(mu_0, mu_1, mu_2)
251 
252     def compute_ap_frequency_dispersion(self):
253         """Compute the resultant distance power spectral density centroidal
        frequency."""
254 
255         mu_0 = self.compute_spectral_moment(0, self.ap_spectral_density[1])
256         mu_1 = self.compute_spectral_moment(1, self.ap_spectral_density[1])
257         mu_2 = self.compute_spectral_moment(2, self.ap_spectral_density[1])
258 
259         return self.compute_frequency_dispersion(mu_0, mu_1, mu_2)
260 
261     def compute_frequency_features(self):
262         """Compute all the frequency features and store them in a
        dictionary."""
263 
264         features = {}
265         features["Total power-RD"] = self.compute_rd_total_power()
266         features["Total power-ML"] = self.compute_ml_total_power()
267         features["Total power-AP"] = self.compute_ap_total_power()
268         features["50% power frequency-RD"] = self.
        compute_rd_power_frequency(50)
269         features["50% power frequency-ML"] = self.
        compute_ml_power_frequency(50)
270         features["50% power frequency-AP"] = self.
        compute_ap_power_frequency(50)
```

```
271         features["80% power frequency-RD"] = self.
    compute_rd_power_frequency(80)
272         features["80% power frequency-ML"] = self.
    compute_ml_power_frequency(80)
273         features["80% power frequency-AP"] = self.
    compute_ap_power_frequency(80)
274         features["95% power frequency-RD"] = self.
    compute_rd_power_frequency(95)
275         features["95% power frequency-ML"] = self.
    compute_ml_power_frequency(95)
276         features["95% power frequency-AP"] = self.
    compute_ap_power_frequency(95)
277         features["Centroidal frequency-RD"] = self.
    compute_rd_centroidal_frequency()
278         features["Centroidal frequency-ML"] = self.
    compute_ml_centroidal_frequency()
279         features["Centroidal frequency-AP"] = self.
    compute_ap_centroidal_frequency()
280         features["Frequency dispersion-RD"] = self.
    compute_rd_frequency_dispersion()
281         features["Frequency dispersion-ML"] = self.
    compute_ml_frequency_dispersion()
282         features["Frequency dispersion-AP"] = self.
    compute_ap_frequency_dispersion()
283 
284         return features
285 
286     def summary(self):
287         """Print out a summary of the frequency features to standard output
    ."""
288 
289         for key, value in self.frequency_features.items():
290             print("{}: {}".format(key, value))
```

Bibliography

[1] Julien Audiffren and Emile Contal. Preprocessing the Nintendo Wii Board Signal to Derive More Accurate Descriptors of Statokinesigrams. *Sensors*, 16(8): 1208, August 2016. ISSN 1424-8220. doi: 10.3390/s16081208. URL http://www.mdpi.com/1424-8220/16/8/1208.

[2] Martina Mancini and Fay B Horak. The relevance of clinical balance assessment tools to differentiate balance deficits. page 17, 2011.

[3] T.E. Prieto, J.B. Myklebust, and B.M. Myklebust. Characterization and modeling of postural steadiness in the elderly: a review. *IEEE Transactions on Rehabilitation Engineering*, 1(1):26–34, March 1993. ISSN 10636528. doi: 10.1109/86.242405. URL http://ieeexplore.ieee.org/document/242405/.

[4] Fay B. Horak. Clinical assessment of balance disorders. *Gait & Posture*, 6(1): 76–84, August 1997. ISSN 09666362. doi: 10.1016/S0966-6362(97)00018-0. URL https://linkinghub.elsevier.com/retrieve/pii/S0966636297000180.

[5] F. Romano, P. Colagiorgio, A. Buizza, F. Sardi, and S. Ramat. Extraction of traditional COP-based features from COM sway in postural stability evaluation. In *2015 37th Annual International Conference of the IEEE Engineering in Medicine and Biology Society (EMBC)*, pages 3715–3718, Milan, August 2015. IEEE. ISBN 978-1-4244-9271-8. doi: 10.1109/EMBC.2015.7319200. URL http://ieeexplore.ieee.org/document/7319200/.

[6] Da Winter. Human balance and posture control during standing and walking. *Gait & Posture*, 3(4):193–214, December 1995. ISSN 09666362. doi: 10.1016/0966-6362(96)82849-9. URL http://linkinghub.elsevier.com/retrieve/pii/0966636296828499.

[7] Luigi Baratto, Pietro G. Morasso, Cristina Re, and Gino Spada. A New Look at Posturographic Analysis in the Clinical Context: Sway-Density versus Other Parameterization Techniques. *Motor Control*, 6(3):246–270, July 2002. ISSN 1087-1640,

1543-2696. doi: 10.1123/mcj.6.3.246. URL http://journals.humankinetics.com/doi/10.1123/mcj.6.3.246.

[8] Marcos Duarte and Sandra M. S. F. Freitas. Revisão sobre posturografia baseada em plataforma de força para avaliação do equilíbrio. *Revista Brasileira de Fisioterapia*, 14(3):183–192, June 2010. ISSN 1413-3555. doi: 10.1590/S1413-35552010000300003. URL http://www.scielo.br/scielo.php?script=sci_arttext&pid=S1413-35552010000300003&lng=pt&nrm=iso&tlng=pt.

[9] S. Mathias, U. S. Nayak, and B. Isaacs. Balance in elderly patients: the "get-up and go" test. *Archives of Physical Medicine and Rehabilitation*, 67(6):387–389, June 1986. ISSN 0003-9993.

[10] M. E. Tinetti. Performance-oriented assessment of mobility problems in elderly patients. *Journal of the American Geriatrics Society*, 34(2):119–126, February 1986. ISSN 0002-8614.

[11] K. Berg, S. Wood-Dauphinee, and J. I. Williams. The Balance Scale: reliability assessment with elderly residents and patients with an acute stroke. *Scandinavian Journal of Rehabilitation Medicine*, 27(1):27–36, March 1995. ISSN 0036-5505.

[12] Ross A. Clark, Adam L. Bryant, Yonghao Pua, Paul McCrory, Kim Bennell, and Michael Hunt. Validity and reliability of the Nintendo Wii Balance Board for assessment of standing balance. *Gait & Posture*, 31(3):307–310, March 2010. ISSN 09666362. doi: 10.1016/j.gaitpost.2009.11.012. URL http://linkinghub.elsevier.com/retrieve/pii/S096663620900664X.

[13] Arnold Huurnink, Duncan P. Fransz, Idsart Kingma, and Jaap H. van Dieën. Comparison of a laboratory grade force platform with a Nintendo Wii Balance Board on measurement of postural control in single-leg stance balance tasks. *Journal of Biomechanics*, 46(7):1392–1395, April 2013. ISSN 00219290. doi: 10.1016/j.jbiomech.2013.02.018. URL http://linkinghub.elsevier.com/retrieve/pii/S0021929013000985.

[14] R. I. Martínez-Lemos, Cárlos Ayán-Pérez, and Sara Bouzas-Rico. Test-retest reliability of the Wii Balance Board for assessing standing balance in young people with intellectual disability. *International Journal of Developmental Disabilities*, pages 1–8, December 2017. ISSN 2047-3869, 2047-3877. doi: 10.1080/20473869.2017.1403065. URL https://www.tandfonline.com/doi/full/10.1080/20473869.2017.1403065.

[15] Bruno Bonnechère, Bart Jansen, Lubos Omelina, Victor Sholukha, and Serge Van Sint Jan. Validation of the Balance Board for Clinical Evaluation of Balance During

Serious Gaming Rehabilitation Exercises. *Telemedicine and e-Health*, 22(9):709–717, September 2016. ISSN 1530-5627, 1556-3669. doi: 10.1089/tmj.2015.0230. URL http://online.liebertpub.com/doi/10.1089/tmj.2015.0230.

[16] Giacomo Severini, Sofia Straudi, Claudia Pavarelli, Marco Da Roit, Carlotta Martinuzzi, Laura Di Marco Pizzongolo, and Nino Basaglia. Use of Nintendo Wii Balance Board for posturographic analysis of Multiple Sclerosis patients with minimal balance impairment. *Journal of NeuroEngineering and Rehabilitation*, 14(1), December 2017. ISSN 1743-0003. doi: 10.1186/s12984-017-0230-5. URL http://jneuroengrehab.biomedcentral.com/articles/10.1186/s12984-017-0230-5.

[17] Renato Monteiro-Junior, Arthur Ferreira, Vivian Puell, Eduardo Lattari, Sérgio Machado, César Otero Vaghetti, and Elirez da Silva. Wii Balance Board: Reliability and Clinical Use in Assessment of Balance in Healthy Elderly Women. *CNS & Neurological Disorders - Drug Targets*, 14(9):1165–1170, November 2015. ISSN 18715273. doi: 10.2174/1871527315666151111120403. URL http://www.eurekaselect.com/openurl/content.php?genre=article&issn=1871-5273&volume=14&issue=9&spage=1165.

[18] Dae-Sung Park and GyuChang Lee. Validity and reliability of balance assessment software using the Nintendo Wii balance board: usability and validation. *Journal of NeuroEngineering and Rehabilitation*, 11(1):99, 2014. ISSN 1743-0003. doi: 10.1186/1743-0003-11-99. URL http://jneuroengrehab.biomedcentral.com/articles/10.1186/1743-0003-11-99.

[19] Brad Hubbard, David Pothier, Cian Hughes, and John Rutka. A Portable, Low-Cost System for Posturography: A Platform for Longitudinal Balance Telemetry. *Journal of Otolaryngology*, 41:5, 2012.

[20] Jeffrey D Holmes, Mary E Jenkins, Andrew M Johnson, Michael A Hunt, and Ross A Clark. Validity of the Nintendo Wii ® balance board for the assessment of standing balance in Parkinson's disease. *Clinical Rehabilitation*, 27(4):361–366, April 2013. ISSN 0269-2155, 1477-0873. doi: 10.1177/0269215512458684. URL http://journals.sagepub.com/doi/10.1177/0269215512458684.

[21] Harrison L. Bartlett, Lena H. Ting, and Jeffrey T. Bingham. Accuracy of force and center of pressure measures of the Wii Balance Board. *Gait & Posture*, 39(1):224–228, January 2014. ISSN 09666362. doi: 10.1016/j.gaitpost.2013.07.010. URL http://linkinghub.elsevier.com/retrieve/pii/S0966636213003184.

[22] Julia Leach, Martina Mancini, Robert Peterka, Tamara Hayes, and Fay Horak. Validating and Calibrating the Nintendo Wii Balance Board to Derive Reliable

Center of Pressure Measures. *Sensors*, 14(10):18244–18267, September 2014. ISSN 1424-8220. doi: 10.3390/s141018244. URL http://www.mdpi.com/1424-8220/14/10/18244.

[23] Francesco Sgrò, Danilo Licari, Roberto Coppola, and Mario Lipoma. ASSESSMENT OF BALANCE ABILITIES IN ELDERLY PEOPLE BY MEANS OF A CLINICAL TEST AND A LOW-COST FORCE PLATE. page 12, 2015.

[24] J. M. Guralnik, E. M. Simonsick, L. Ferrucci, R. J. Glynn, L. F. Berkman, D. G. Blazer, P. A. Scherr, and R. B. Wallace. A Short Physical Performance Battery Assessing Lower Extremity Function: Association With Self-Reported Disability and Prediction of Mortality and Nursing Home Admission. *Journal of Gerontology*, 49(2):M85–M94, March 1994. ISSN 0022-1422. doi: 10.1093/geronj/49.2.M85. URL https://academic.oup.com/geronj/article-lookup/doi/10.1093/geronj/49.2.M85.

[25] Bruno Bonnechère, Bart Jansen, Lubos Omelina, Marcel Rooze, and Serge Van Sint Jan. Interchangeability of the Wii Balance Board for Bipedal Balance Assessment. *JMIR Rehabilitation and Assistive Technologies*, 2(2):e8, August 2015. ISSN 2369-2529. doi: 10.2196/rehab.3832. URL http://rehab.jmir.org/2015/2/e8/.

[26] Bruno Bonnechère, Bart Jansen, Lubos Omelina, Marcel Rooze, and Serge Van Sint Jan. Validation of the Balance Board^{TM} for Clinical Evaluation of Balance Through Different Conditions. In Habib M. Fardoun, Victor M R. Penichet, and Daniyal M. Alghazzawi, editors, *ICTs for Improving Patients Rehabilitation Research Techniques*, volume 515, pages 11–23. Springer Berlin Heidelberg, Berlin, Heidelberg, 2015. ISBN 978-3-662-48644-3 978-3-662-48645-0. doi: 10.1007/978-3-662-48645-0_2. URL http://link.springer.com/10.1007/978-3-662-48645-0_2.

[27] Kazuki Yoshikawa, Takehito Kojima, Akihiro Sugiura, and Masaru Miyao. Possibility of Using the Wii Balance Board in Stabilometry. *Forma*, 2015. ISSN 09116036, 21891311. doi: 10.5047/forma.2015.001. URL http://www.scipress.org/journals/forma/abstract/3001/30010001.html.

[28] Letizia Castelli, Luca Stocchi, Maurizio Patrignani, Giovanni Sellitto, Manuela Giuliani, and Luca Prosperini. We-Measure: Toward a low-cost portable posturography for patients with multiple sclerosis using the commercial Wii balance board. *Journal of the Neurological Sciences*, 359(1-2):440–444, December 2015. ISSN 1878-5883. doi: 10.1016/j.jns.2015.10.016.

[29] Julien Audiffren, Ioannis Bargiotas, Nicolas Vayatis, Pierre-Paul Vidal, and Damien Ricard. A Non Linear Scoring Approach for Evaluating Balance: Classification of

Elderly as Fallers and Non-Fallers. *PLOS ONE*, 11(12):e0167456, December 2016. ISSN 1932-6203. doi: 10.1371/journal.pone.0167456. URL https://dx.plos.org/10.1371/journal.pone.0167456.

[30] Ladan Zakeri, Ali Asghar Jamebozorgi, and Amir Hossein Kahlaee. Correlation Between Center of Pressure Measures Driven from Wii Balance Board and Force Platform. *Asian Journal of Sports Medicine*, In Press(In Press), July 2017. ISSN 2008-000X, 2008-7209. doi: 10.5812/asjsm.55436. URL http://asjsm.neoscriber.org/en/articles/55436.html.

[31] O. Van Hove, A. Van Muylem, D. Leduc, B. Jansen, V. Feipel, S. Van Sint Jan, and B. Bonnechère. Validation of the Wii Balance Board to assess balance modifications induced by increased respiratory loads in healthy subjects. *Gait & Posture*, 68:449–452, February 2019. ISSN 0966-6362. doi: 10.1016/j.gaitpost.2018.12.033. URL http://www.sciencedirect.com/science/article/pii/S0966636218314334.

[32] Ross A. Clark, Benjamin F. Mentiplay, Yong-Hao Pua, and Kelly J. Bower. Reliability and validity of the Wii Balance Board for assessment of standing balance: A systematic review. *Gait & Posture*, 61:40–54, March 2018. ISSN 0966-6362. doi: 10.1016/j.gaitpost.2017.12.022. URL http://www.sciencedirect.com/science/article/pii/S0966636217310512.

[33] Arnaud Barre and Stéphane Armand. Biomechanical ToolKit: Open-source framework to visualize and process biomechanical data. *Computer Methods and Programs in Biomedicine*, 114(1):80–87, April 2014. ISSN 01692607. doi: 10.1016/j.cmpb.2014.01.012. URL https://linkinghub.elsevier.com/retrieve/pii/S0169260714000248.

[34] T.E. Prieto, J.B. Myklebust, R.G. Hoffmann, E.G. Lovett, and B.M. Myklebust. Measures of postural steadiness: differences between healthy young and elderly adults. *IEEE Transactions on Biomedical Engineering*, 43(9):956–966, September 1996. ISSN 00189294. doi: 10.1109/10.532130. URL http://ieeexplore.ieee.org/document/532130/.

[35] Lion Krischer. Mtspec Python Wrappers 0.3.2, August 2016. URL https://zenodo.org/record/321789.

[36] G.A. Prieto, R.L. Parker, and F.L. Vernon III. A Fortran 90 library for multitaper spectrum analysis. *Computers & Geosciences*, 35(8):1701–1710, August 2009. ISSN 00983004. doi: 10.1016/j.cageo.2008.06.007. URL https://linkinghub.elsevier.com/retrieve/pii/S0098300409000077.

[37] P. P. N. de Groen. An Introduction to Total Least Squares. *arXiv:math/9805076*, May 1998. URL http://arxiv.org/abs/math/9805076. arXiv: math/9805076.

[38] J Martin Bland and Douglas G Altman. STATISTICAL METHODS FOR ASSESSING AGREEMENT BETWEEN TWO METHODS OF CLINICAL MEASUREMENT. page 9.

[39] Davide Giavarina. Understanding Bland Altman analysis. *Biochemia Medica*, 25 (2):141–151, 2015. ISSN 18467482. doi: 10.11613/BM.2015.015. URL http://www.biochemia-medica.com/en/journal/25/2/10.11613/BM.2015.015.

[40] Terry K. Koo and Mae Y. Li. A Guideline of Selecting and Reporting Intraclass Correlation Coefficients for Reliability Research. *Journal of Chiropractic Medicine*, 15(2):155–163, June 2016. ISSN 15563707. doi: 10.1016/j.jcm.2016.02.012. URL https://linkinghub.elsevier.com/retrieve/pii/S1556370716000158.

[41] Christoph Maurer and Robert J. Peterka. A New Interpretation of Spontaneous Sway Measures Based on a Simple Model of Human Postural Control. *Journal of Neurophysiology*, 93(1):189–200, January 2005. ISSN 0022-3077, 1522-1598. doi: 10.1152/jn.00221.2004. URL http://www.physiology.org/doi/10.1152/jn.00221.2004.

[42] José Magalhães de Oliveira. Statokinesigram normalization method. *Behavior Research Methods*, 49(1):310–317, February 2017. ISSN 1554-3528. doi: 10.3758/s13428-016-0706-4. URL http://link.springer.com/10.3758/s13428-016-0706-4.

[43] Ryo Eguchi and Masaki Takahashi. Validity of the Nintendo Wii Balance Board for Kinetic Gait Analysis. *Applied Sciences*, 8(2):285, February 2018. ISSN 2076-3417. doi: 10.3390/app8020285. URL http://www.mdpi.com/2076-3417/8/2/285.

[44] Alessandro Mengarelli, Federica Verdini, Stefano Cardarelli, Francesco Di Nardo, Laura Burattini, and Sandro Fioretti. Balance assessment during squatting exercise: A comparison between laboratory grade force plate and a commercial, low-cost device. *Journal of Biomechanics*, 71:264–270, April 2018. ISSN 0021-9290. doi: 10.1016/j.jbiomech.2018.01.029. URL http://www.sciencedirect.com/science/article/pii/S0021929018300605.

[45] A. Mengarelli, S. Cardarelli, A. Strazza, F. Di Nardo, S. Fioretti, and F. Verdini. Validity of the Nintendo Wii Balance Board for the Assessment of Balance Measures in the Functional Reach Test. *IEEE Transactions on Neural Systems and Rehabilitation Engineering*, 26(7):1400–1406, July 2018. ISSN 1534-4320. doi: 10.1109/TNSRE.2018.2843884.

[46] James Lee, Graham Webb, Adam P. Shortland, Rebecca Edwards, Charlotte Wilce, and Gareth D. Jones. Reliability and feasibility of gait initiation centre-of-pressure excursions using a Wii® Balance Board in older adults at risk of falling. *Aging Clinical and Experimental Research*, 31(2):257–263, February 2019. ISSN 1720-8319. doi: 10.1007/s40520-018-0945-6. URL https://doi.org/10.1007/s40520-018-0945-6.

[47] Marcelo Guimarães Silva, Pedro Vieira Sarmet Moreira, and Henrique Martins Rocha. Development of a low cost force platform for biomechanical parameters analysis. *Research on Biomedical Engineering*, 33(3):259–268, September 2017. ISSN 2446-4740, 2446-4732. doi: 10.1590/2446-4740.01217. URL http://www.scielo.br/scielo.php?script=sci_arttext&pid=S2446-47402017000300259&lng=en&tlng=en.